Supporting Information Section

Inhibitory and Cooperative Effects Regulated by pH in Host-Guest Complexation Between Cationic Pillar[5]arene and Reactive 2-Carboxyphthalanilic Acid

Eduardo V. Silveira,*,† Vanessa Nascimento,†† Eduardo H. Wanderlind,† Ricardo F. Affeldt,*,† Gustavo A. Micke,† Luis Garcia-Rio, ††† and Faruk Nome.†

†Departamento de Química, Universidade Federal de Santa Catarina, Florianópolis – SC, 88040-900, Brazil.

††Departamento de Química Orgânica, Universidade Federal Fluminense, Niterói – RJ, 24020-150, Brazil.

†††Centro de Investigación en Química Biolóxica e Materiais Moleculares (CiQUS), Departamento de Química Física, Universidade de Santiago de Compostela, 15782, Santiago de Compostela, Spain.

Section

1. Synthetic schemes

Schemes S1 and S2 show the synthetic routes used to obtain the 2-carboxyphthalanilic acid (CPA) and pillararenes (P5A and P6A), respectively.

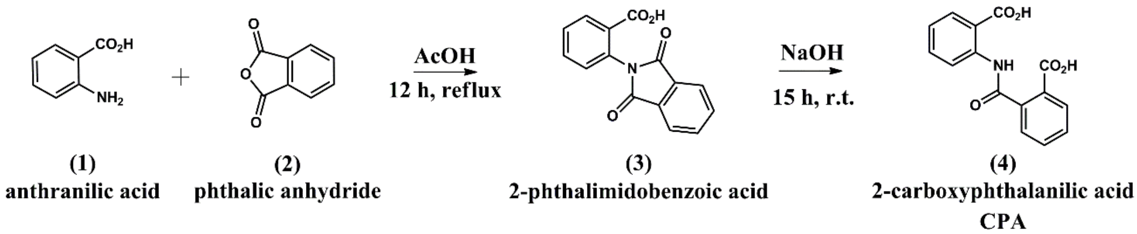

Scheme S1 – Synthetic route to obtain CPA.

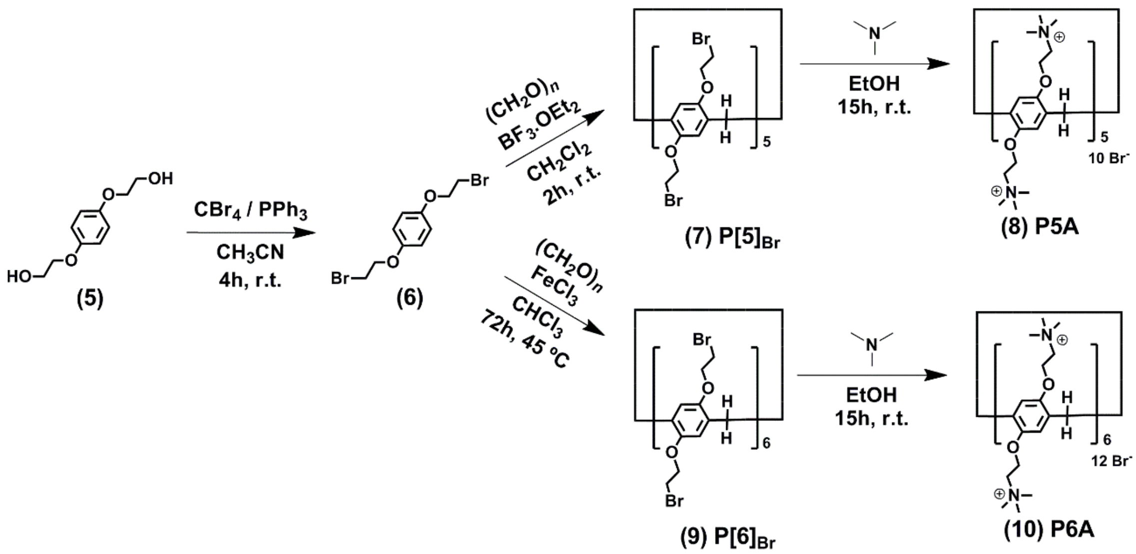

Scheme S2 – Synthetic routes to obtain P5A and P6A.

2. ^{1}H and $^{13}C\{^{1}H\}$ NMR spectra

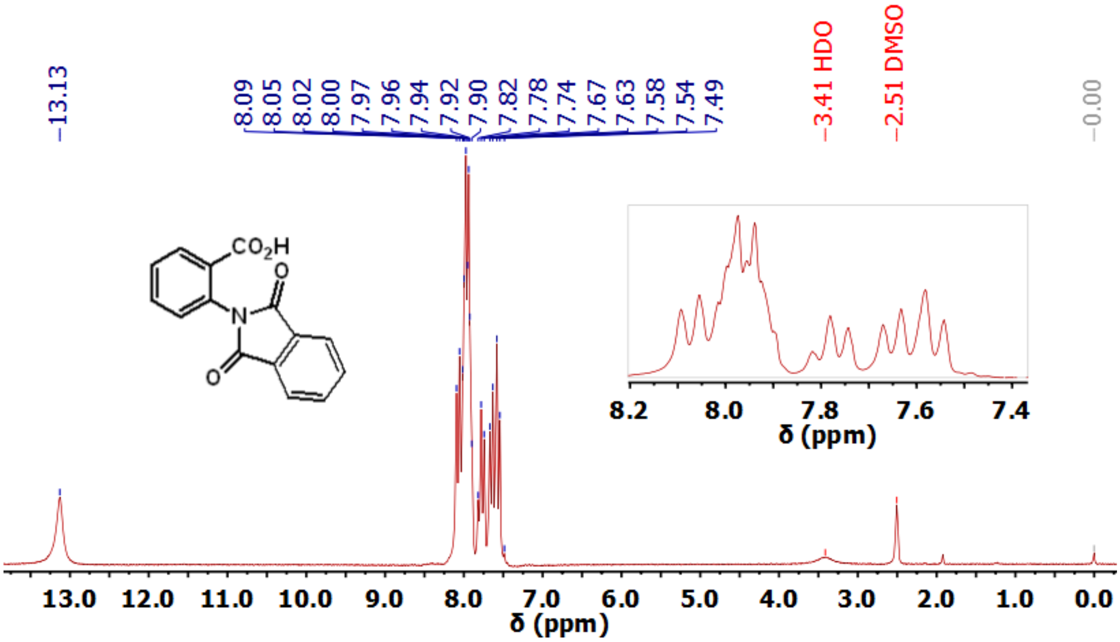

Figure S1a – ^{1}H NMR spectrum of compound **3** (DMSO-D_6; 200 MHz; 25.0 ºC; TMS).

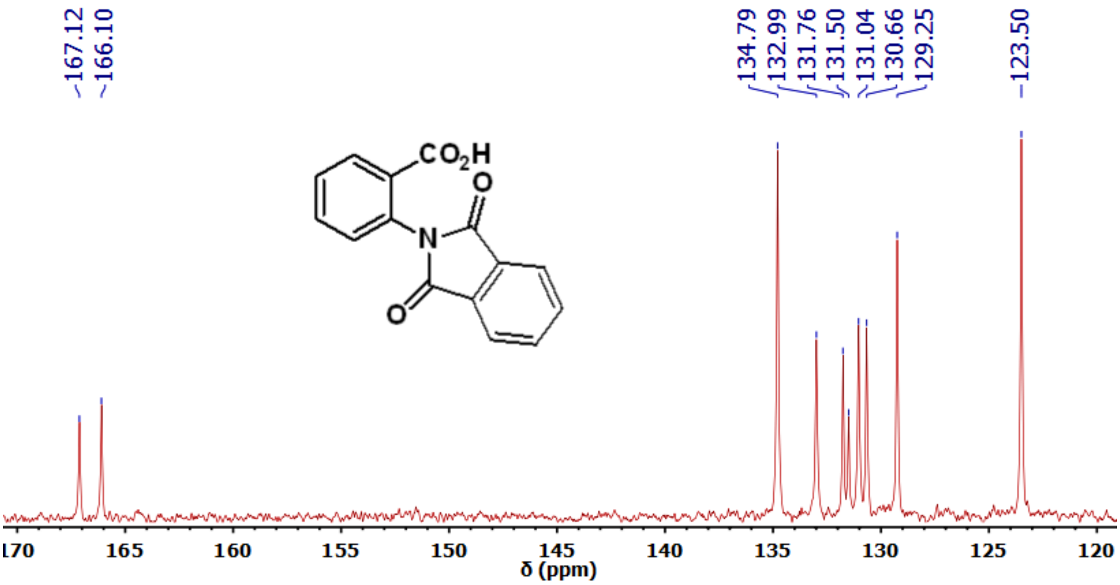

Figure S1b – $^{13}C\{^{1}H\}$ NMR spectrum of compound **3** (DMSO-D_6; 50 MHz; 25.0 ºC; residual solvent as reference).

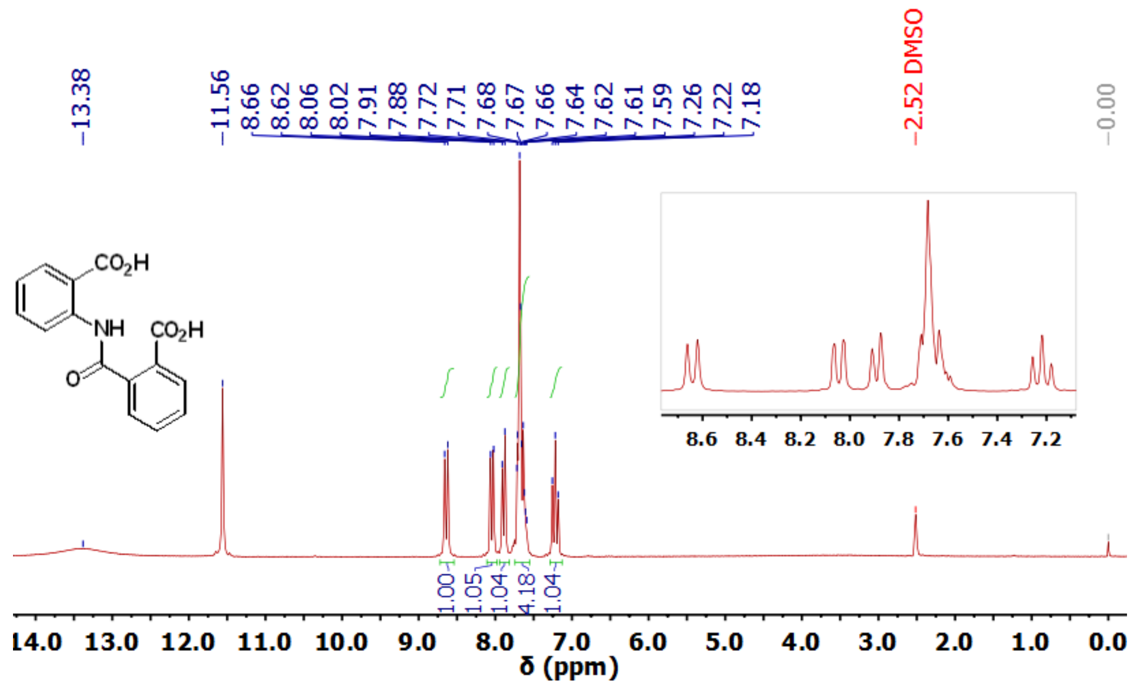

Figure S2a – ^{1}H NMR spectrum of compound **4** (CPA) (DMSO-D$_6$; 200 MHz; 25.0 ºC; TMS).

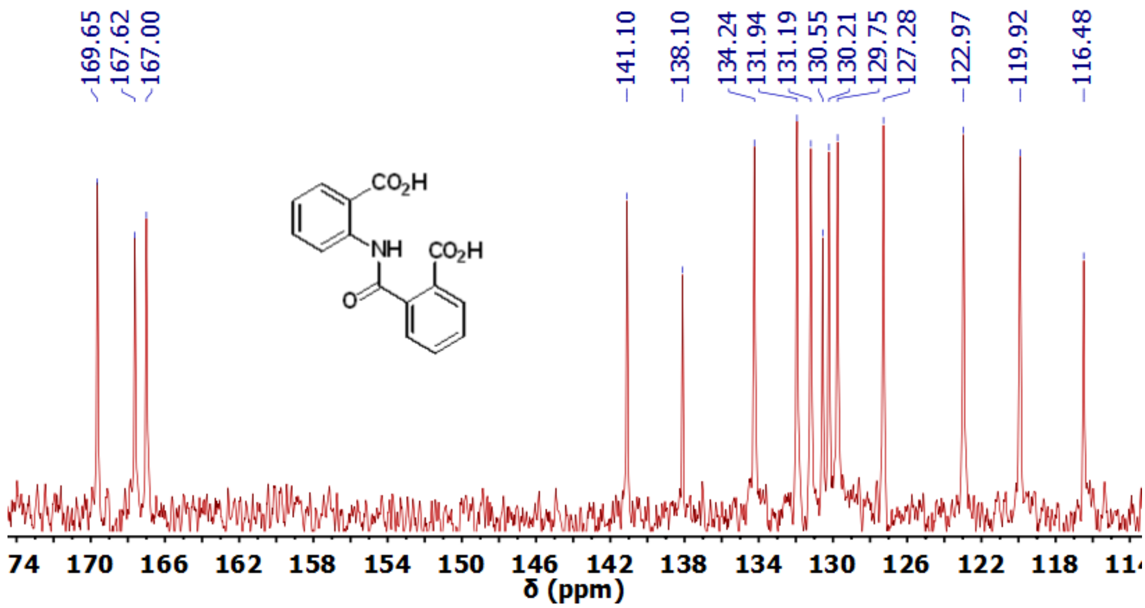

Figure S2b – ^{13}C{^{1}H} NMR spectrum of compound **4** (CPA) (DMSO-D$_6$; 50 MHz; 25.0 ºC; residual solvent as reference).

3. HRMS/ESI-TOF spectra

The HRMS spectra of pillararenes were recorded by using a Bruker Daltonics – micrOTOF-Q II/ESI-Qq-TOF mass spectrometer.

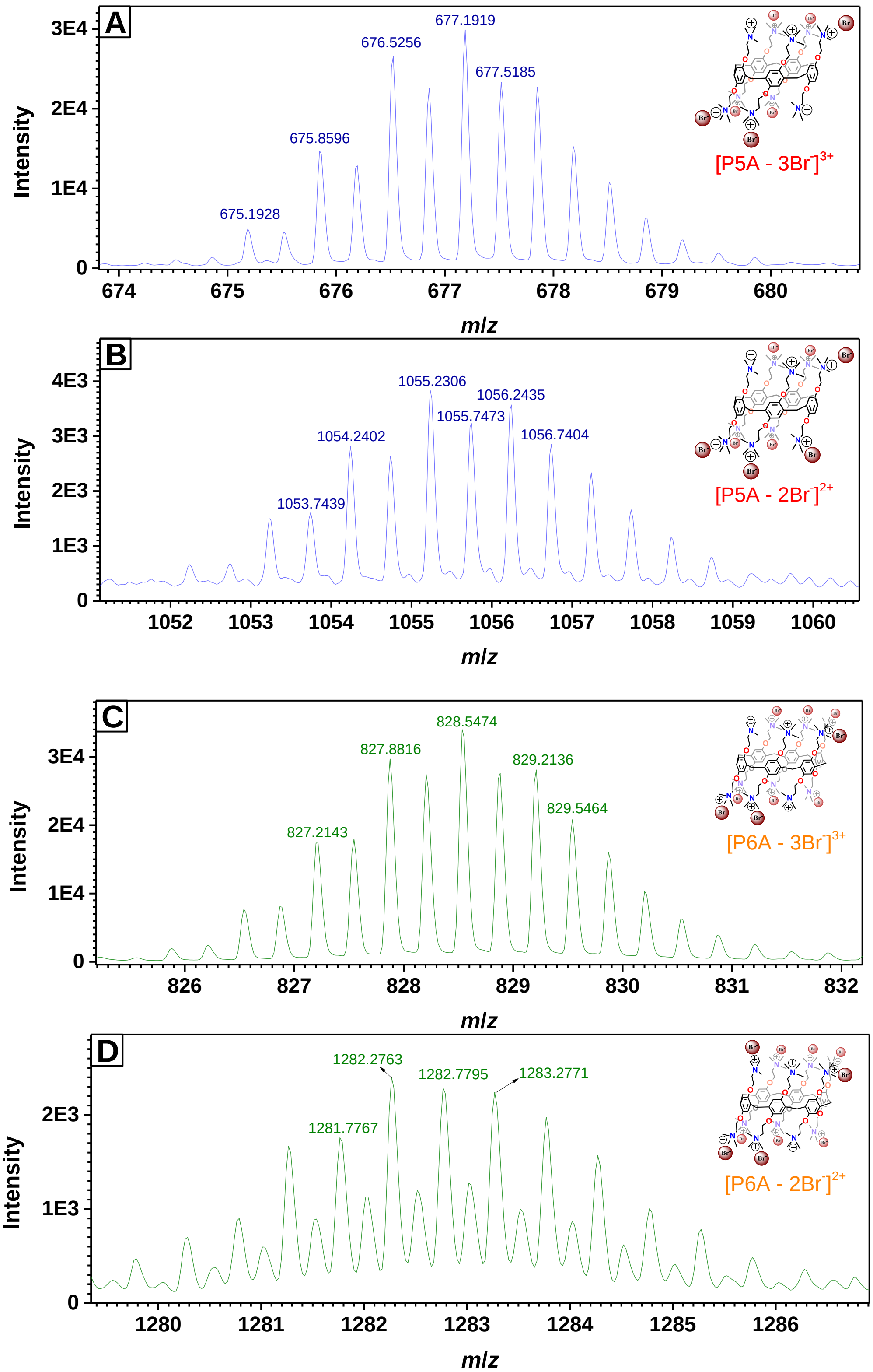

Figure S3 – HRMS/ESI-TOF spectra of aqueous solutions of P5A (**A** and **B**) and P6A (**C** and **D**) in positive ion mode.

4. Product characterization

(1) ^{1}H NMR: The products were first confirmed by the comparison between **A** and **B** spectra (Figure S4), corresponding to the aqueous solutions of the fully hydrolyzed CPA (25.5 mM) and a mixture of anthranilic acid (28.50 mM) and phthalic anhydride (23.31 mM), respectively. For confirmation, to the same samples acetonitrile was added to observe the variation of the chemical shifts of the aromatic protons (**C** and **D** spectra).

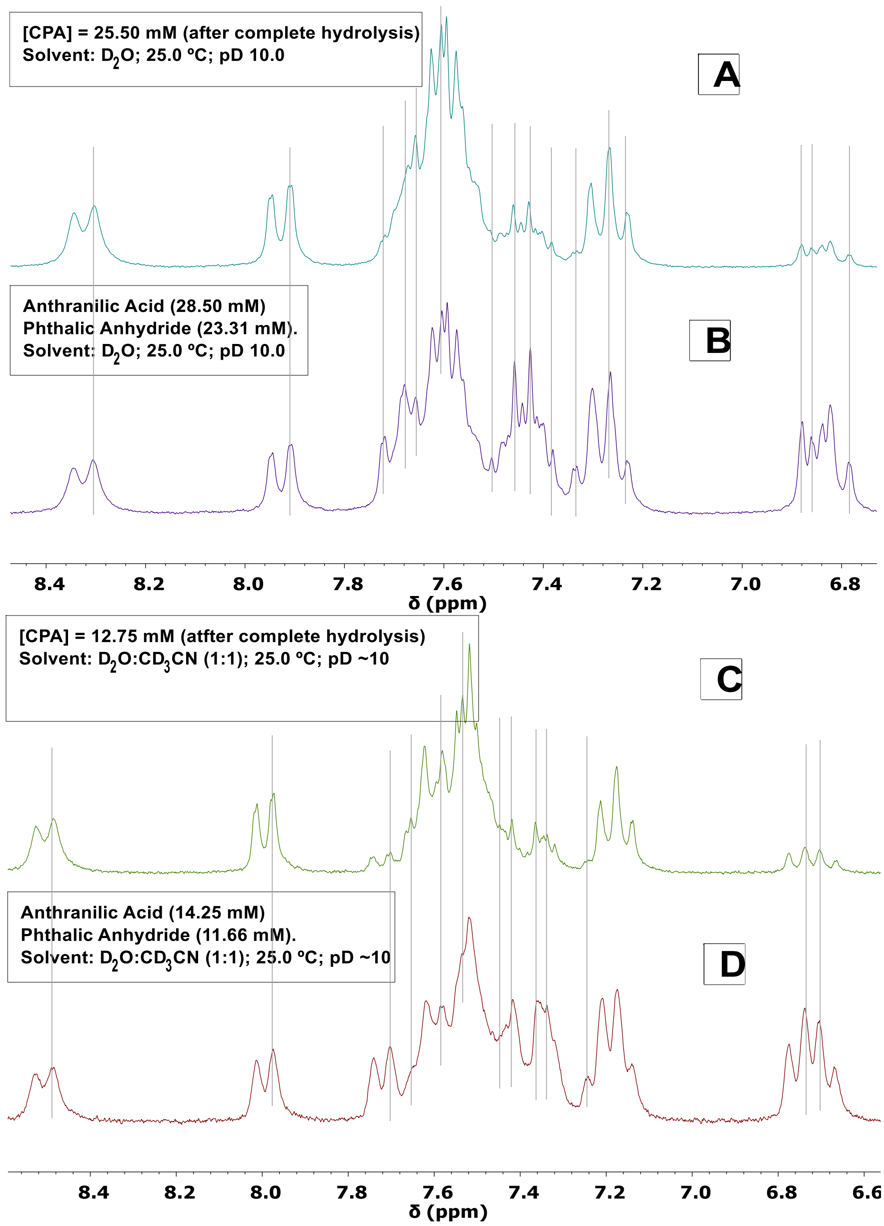

Figure S4 – ^{1}H NMR spectra of aqueous solutions of fully hydrolyzed CPA (**A**) and a mixture of anthranilic acid and phthalic anhydride (**B**). Acetonitrile was added to hydrolyzed CPA (**C**) and to the mixture of anthranilic acid and phthalic anhydride (**D**). (200 MHz; 25.0 °C; TMSP).

(2) Capillary Electrophoresis/DAD-UV (CE): The products were also confirmed by CE analysis using an Agilent HP 3D Capillary Electrophoresis system with a UV-Vis diode-array detector set at 214 nm (25 ºC and pH 9.5), as shown in Figure S5.

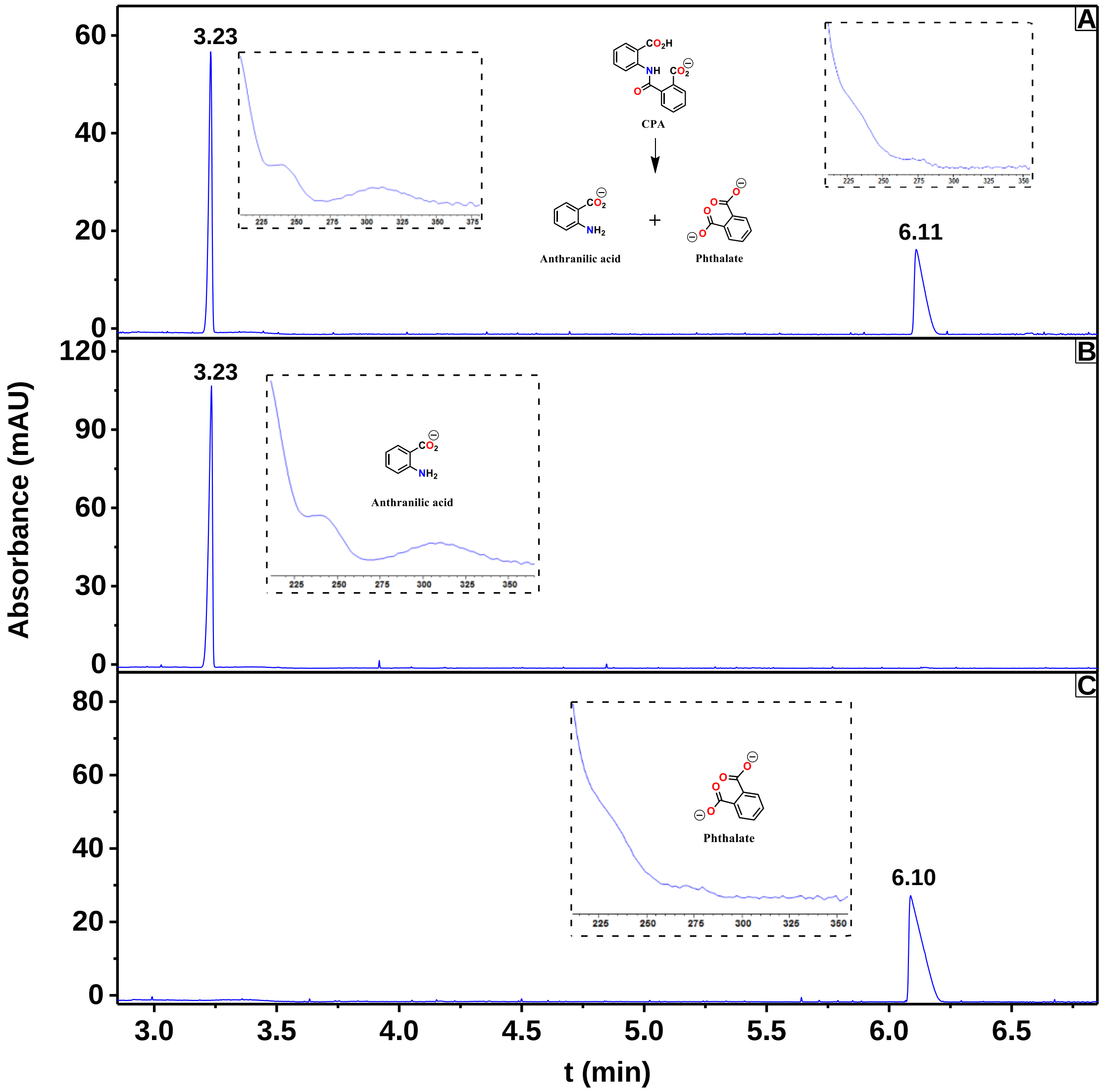

Figure S5 – CZE/DAD-UV electropherogram of fully hydrolyzed CPA (**A**), anthranilic acid (**B**) and phthalic anhydride (**C**), at 25 ºC and pH 9.5.

5. Kinetic data

Table S1 shows the kinetic data for the CPA decomposition in the presence of P5A as a function of the pH (Figure 1A in the manuscript, green data), and Table 2 presents the k_{obs} values for the rate-concentration profiles at different pH values. (Figure 2A-D in the manuscript). The UV/Vis spectra and the absorbance *vs*. time profiles from which the k_{obs} values were calculated are present sequentially. For the kinetics at higher pHs, the k_{obs} values were calculated by the initial velocity method. All k_{obs} were determined by appearance of the anthranilic acid at 330-350 nm. Positively ionizable buffers were preferred for use in the experiments to minimize the electrostatic interactions with pillararenes: HEPES, aniline and Bis-Tris methane. Experiments at four different buffer concentrations (10 mM; 20 mM; 30 mM and 40 mM) were performed to subtract their effects on k_{obs}. For this, the buffer concentrations were extrapolated up to 0 mM to obtain the exact k_{obs} of CPA decomposition inside the cavity of the pillararenes.

Table S1. Influence of pH on the k_{obs} for CPA decomposition in P5A cavity ([CPA] = 1.0 × 10^{-4} M^{-1}; ([P5A] = 4.0 × 10^{-4} M^{-1}; 25.0 ºC).

pH	**k_{obs} (s^{-1})**
1.56	(2.28 ± 0.05) × 10^{-4}
1.80	(2.23 ± 0.05) × 10^{-4}
2.03	(2.11 ± 0.06) × 10^{-4}
2.22	(1.90 ± 0.06) × 10^{-4}
2.49	(1.38 ± 0.06) × 10^{-4}
2.76	(9.93 ± 0.08) × 10^{-5}
3.06	(5.48 ± 0.08) × 10^{-5}
3.27	(3.26 ± 0.06) × 10^{-5}
3.64	(9.99 ± 0.05) × 10^{-6}
4.02	(3.87 ± 0.05) × 10^{-6}
4.49	(1.52 ± 0.06) × 10^{-6}
4.99	(3.08 ± 0.07) × 10^{-7}
5.68	(6.71 ± 0.08) × 10^{-8}
6.40	(1.35 ± 0.08) × 10^{-8}

Table S2. Influence of P5A concentration on the k_{obs} for CPA decomposition at different pHs ([CPA] = 1.0 × 10^{-4} M^{-1}; 25.0 ºC).

P5A, M	**k_{obs} (s^{-1})**			
	pH 2.50	**pH 3.45**	**pH 4.25**	**pH 6.00**
0	(5.66 ± 0.05) × 10^{-4}	(1.41 ± 0.10) × 10^{-3}	(1.30 ± 0.16) × 10^{-3}	(1.73 ± 0.11) × 10^{-5}
1.20 × 10^{-6}	(5.50 ± 0.10) × 10^{-4}	(1.28 ± 0.16) × 10^{-3}	(1.22 ± 0.20) × 10^{-3}	--
2.00 × 10^{-6}	---	---	---	(1.65 ± 0.02) × 10^{-5}
4.00 × 10^{-6}	(5.47 ± 0.07) × 10^{-4}	(1.10 ± 0.25) × 10^{-3}	(1.03 ± 0.20) × 10^{-3}	---
6.00 × 10^{-6}	(5.32 ± 0.07) × 10^{-4}	(9.79 ± 0.31) × 10^{-4}	(9.18 ± 0.23) × 10^{-4}	(1.41 ± 0.03) × 10^{-5}
8.00 × 10^{-6}	(5.25 ± 0.08) × 10^{-4}	(8.22 ± 0.35) × 10^{-4}	(8.54 ± 0.31) × 10^{-4}	---
1.00 × 10^{-5}	(5.14 ± 0.08) × 10^{-4}	(7.80 ± 0.36) × 10^{-4}	(7.58 ± 0.35) × 10^{-4}	---
2.00 × 10^{-5}	---	---	---	(9.14 ± 0.12) × 10^{-6}
3.00 × 10^{-5}	(4.37 ± 0.07) × 10^{-4}	(4.50 ± 0.05) × 10^{-4}	(1.81 ± 0.05) × 10^{-4}	---
4.00 × 10^{-5}	---	---	---	(3.98 ± 0.12) × 10^{-6}
5.00 × 10^{-5}	(3.82 ± 0.08) × 10^{-4}	(2.03 ± 0.03) × 10^{-4}	(7.02 ± 0.10) × 10^{-5}	---
6.00 × 10^{-5}	---	---	---	(2.39 ± 0.08) × 10^{-6}
8.00 × 10^{-5}	(3.36 ± 0.11) × 10^{-4}	(7.62 ± 0.05) × 10^{-5}	(1.42 ± 0.10) × 10^{-5}	(1.23 ± 0.05) × 10^{-6}
1.00 × 10^{-4}	(3.13 ± 0.05) × 10^{-4}	(6.01 ± 0.05) × 10^{-5}	(8,70 ± 0.13) × 10^{-6}	(7.37 ± 0.07) × 10^{-7}
2.00 × 10^{-4}	---	---	---	(2.00 ± 0.07) × 10^{-7}
3.00 × 10^{-4}	(2.23 ± 0.07) × 10^{-4}	(2.27 ± 0.05) × 10^{-5}	(2.99 ± 0.14) × 10^{-6}	---
4.00 × 10^{-4}	---	---	---	(9.09 ± 0.07) × 10^{-8}
5.00 × 10^{-4}	(1.98 ± 0.05) × 10^{-4}	---	---	---
8.00 × 10^{-4}	(1.80 ± 0.05) × 10^{-4}	(1.96 ± 0.07) × 10^{-5}	(2.45 ± 0.14) × 10^{-6}	(7.80 ± 0.06) × 10^{-8}
1.20 × 10^{-3}	---	---	---	(7.13 ± 0.24) × 10^{-8}
1.50 × 10^{-3}	(1.50 ± 0.07) × 10^{-4}	---	(2.42 ± 0.12) × 10^{-6}	---
2.00 × 10^{-3}	(1.44 ± 0.07) × 10^{-4}	(1.91 ± 0.08) × 10^{-5}	(2.48 ± 0.12) × 10^{-6}	---

UV/Vis spectra

pH-rate profile of CPA decomposition in P5A cavity

- **pH 1.56**

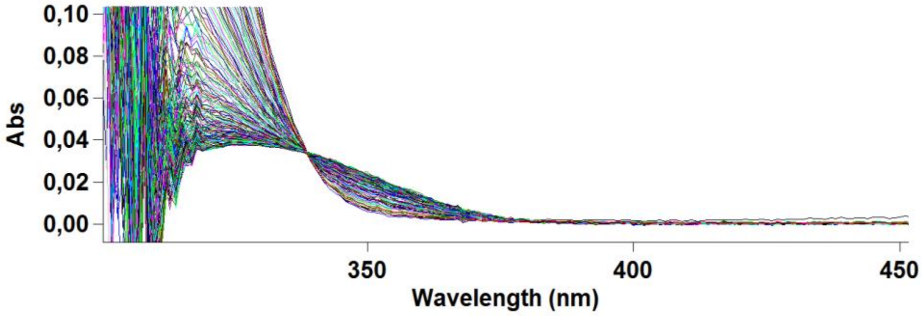

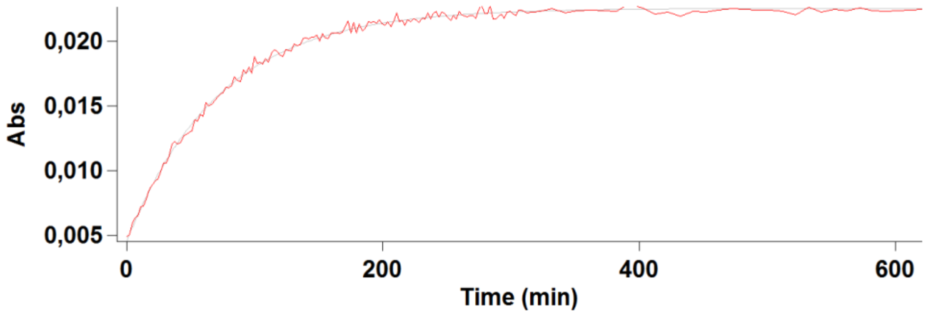

- **pH 1.80**

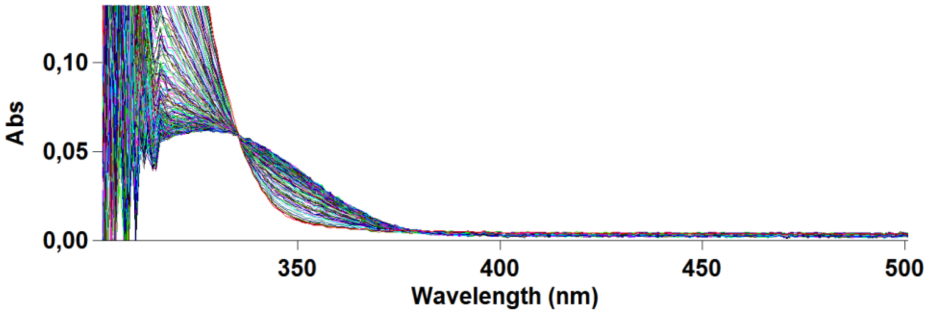

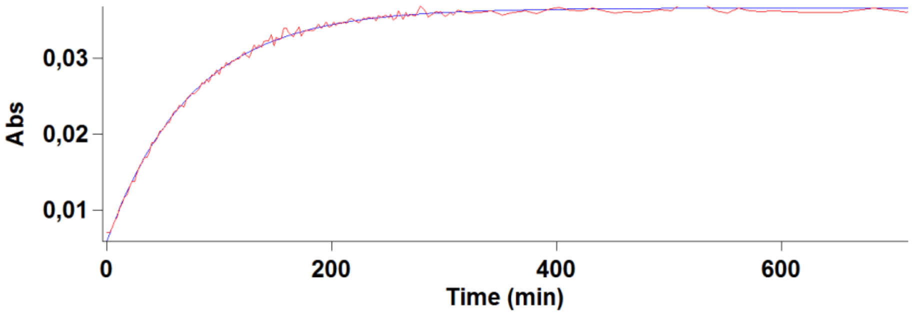

- **pH 2.03**

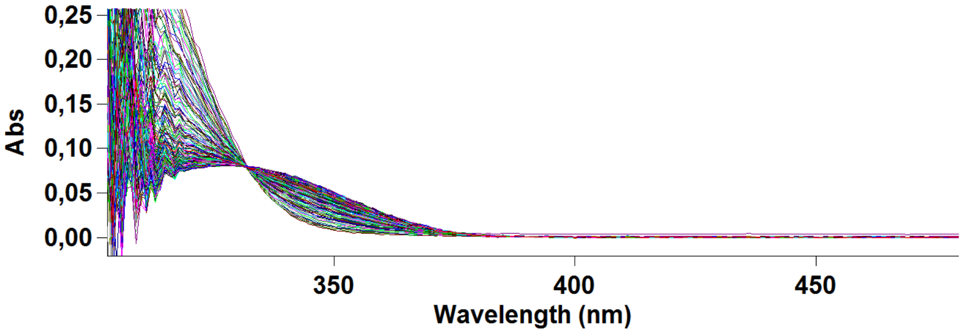
0,25
0,20
0,15
0,10
0,05
0,00
Abs
350
400
450
Wavelength (nm)

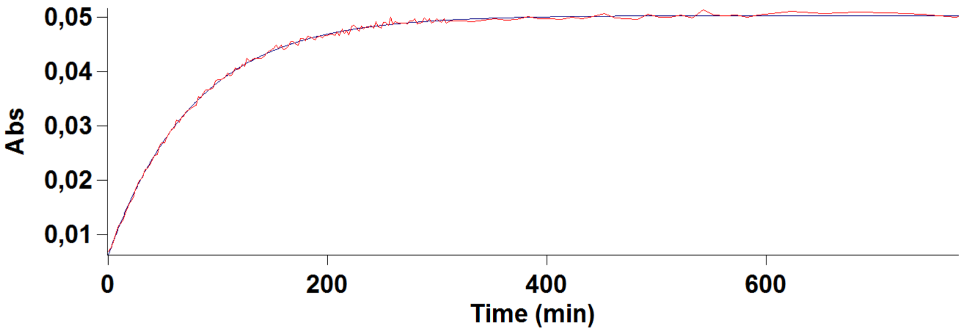
0,05
0,04
0,03
0,02
0,01
Abs
0
200
400
600
Time (min)

- **pH 2.22**

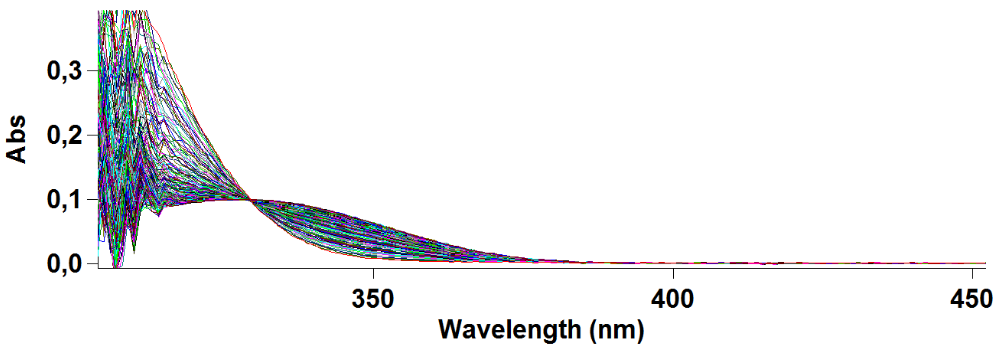
0,3
0,2
0,1
0,0
Abs
350
400
450
Wavelength (nm)

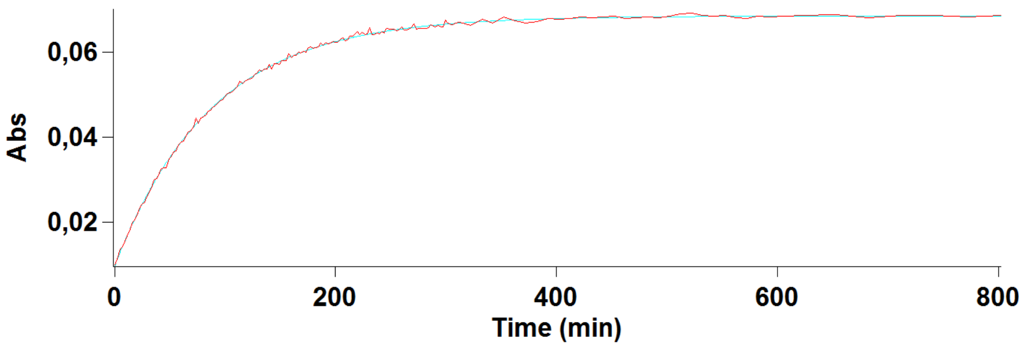
0,06
0,04
0,02
Abs
0
200
400
600
800
Time (min)

- **pH 2.49**

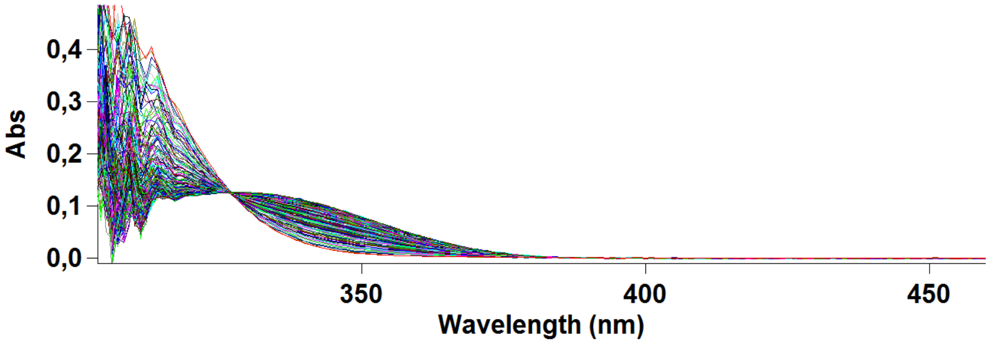

Abs
0,4
0,3
0,2
0,1
0,0
350
400
450
Wavelength (nm)

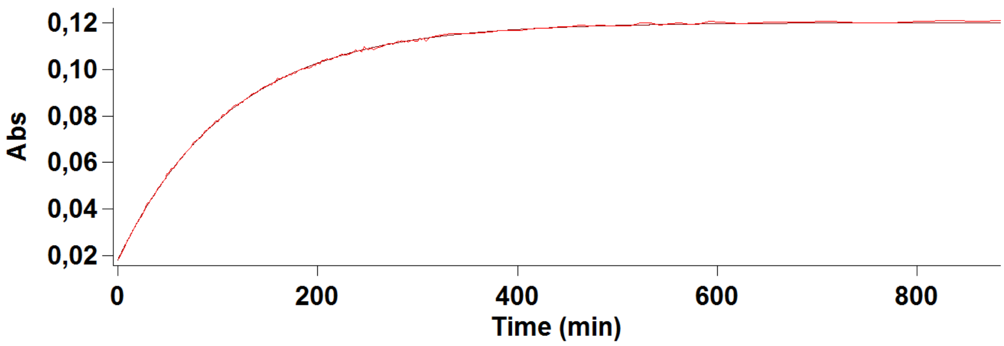

Abs
0,12
0,10
0,08
0,06
0,04
0,02
0
200
400
600
800
Time (min)

- **pH 2.76**

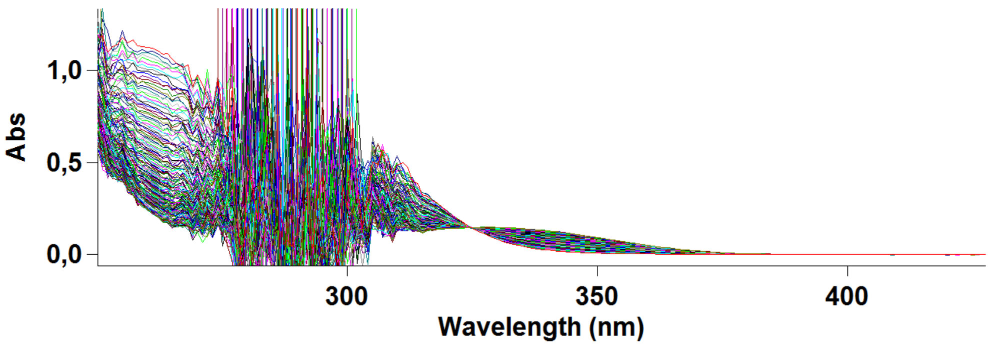

Abs
1,0
0,5
0,0
300
350
400
Wavelength (nm)

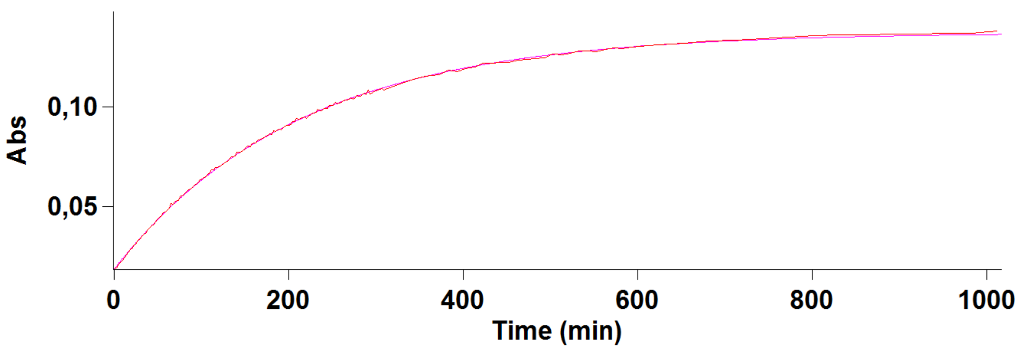

Abs
0,10
0,05
0
200
400
600
800
1000
Time (min)

- **pH 3.06**

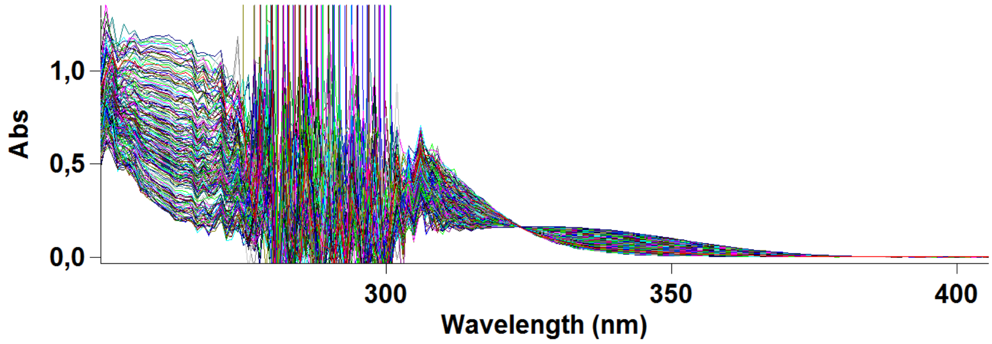

1,0
0,5
0,0
Abs
300
350
400
Wavelength (nm)

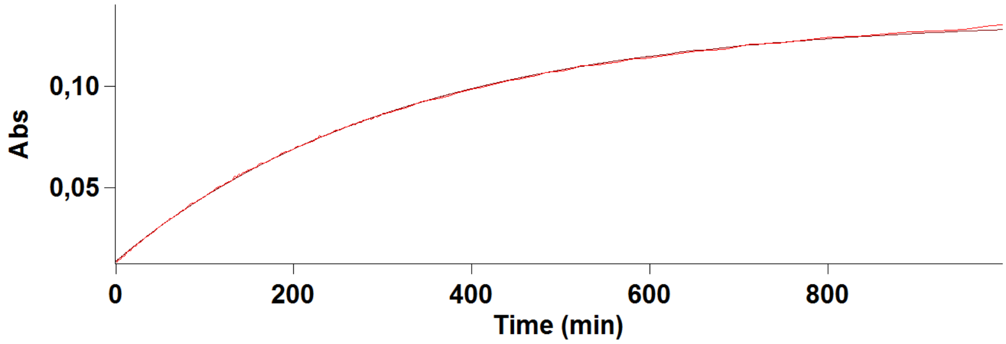

0,10
0,05
Abs
0
200
400
600
800
Time (min)

- **pH 3.27**

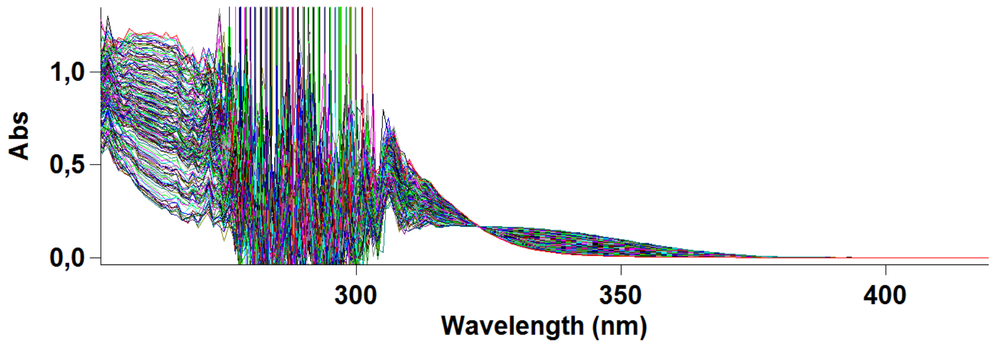

1,0
0,5
0,0
Abs
300
350
400
Wavelength (nm)

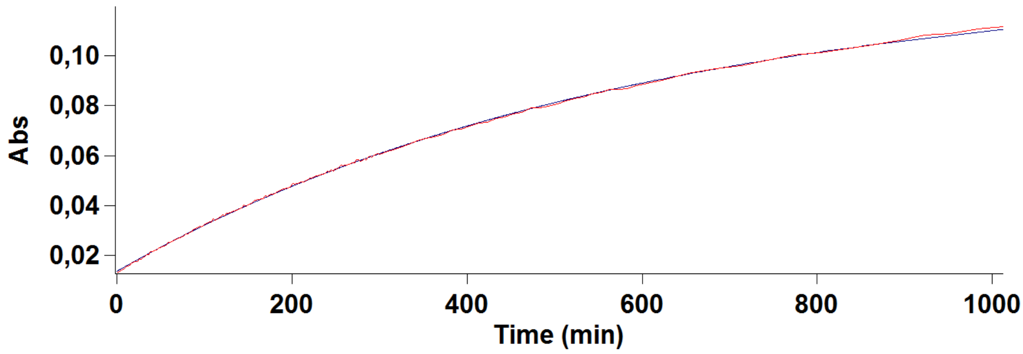

0,10
0,08
0,06
0,04
0,02
Abs
0
200
400
600
800
1000
Time (min)

- **pH 3.64**

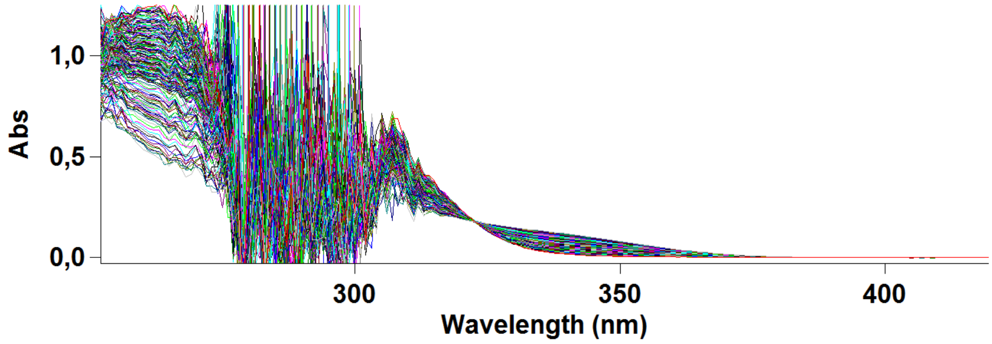
1,0
0,5
0,0
Abs
300
350
400
Wavelength (nm)

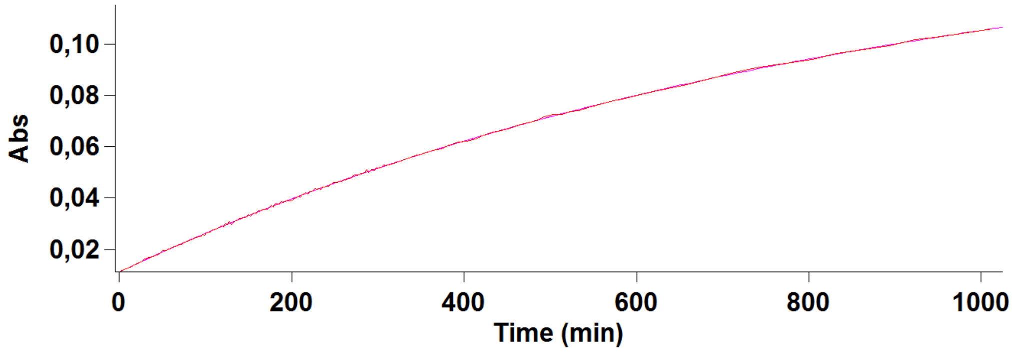
0,10
0,08
0,06
0,04
0,02
Abs
0
200
400
600
800
1000
Time (min)

- **pH 4.02**

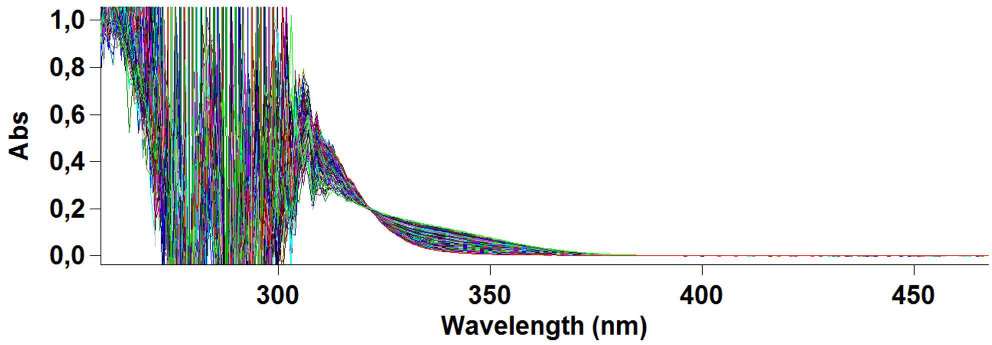
1,0
0,8
0,6
0,4
0,2
0,0
Abs
300
350
400
450
Wavelength (nm)

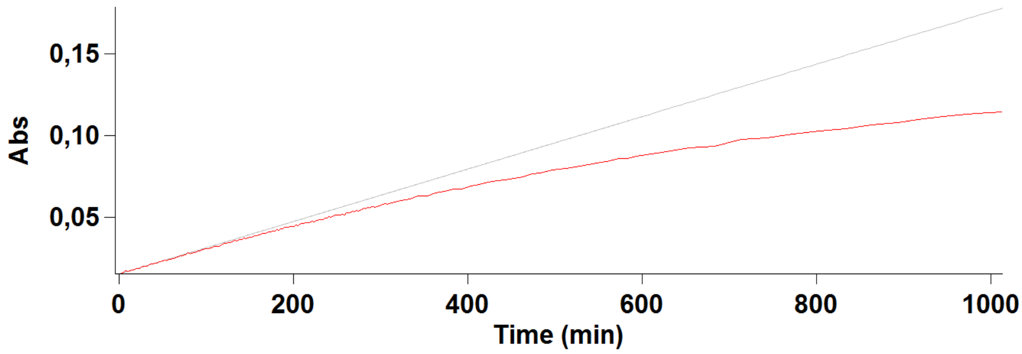
0,15
0,10
0,05
Abs
0
200
400
600
800
1000
Time (min)

- **pH 4.49**

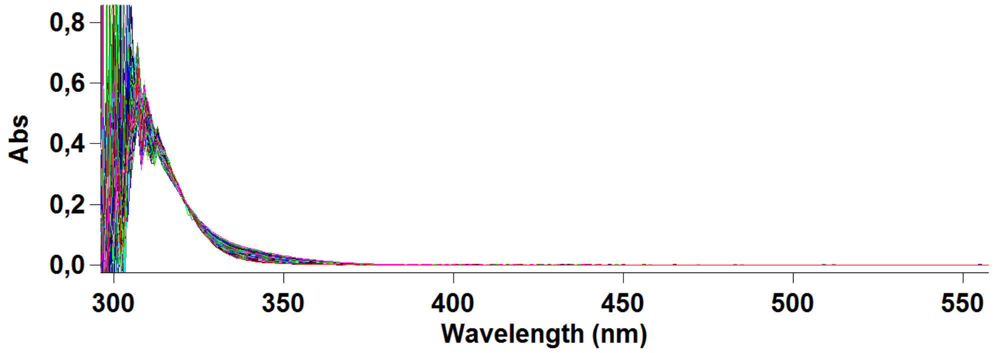
0,8
0,6
0,4
0,2
0,0
Abs
300
350
400
450
500
550
Wavelength (nm)

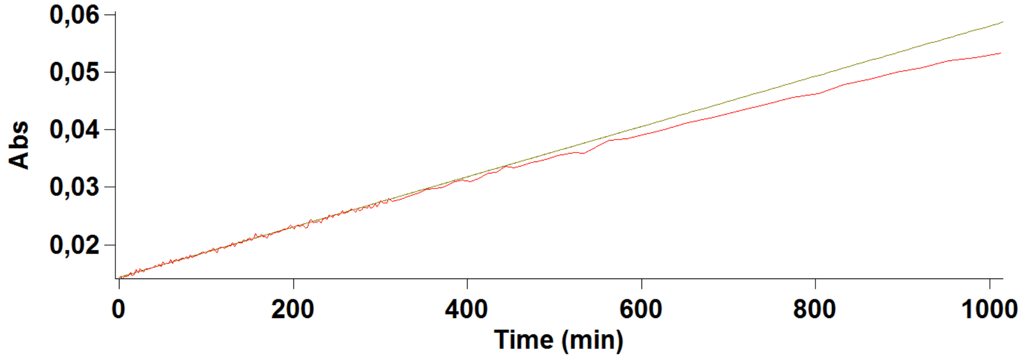
0,06
0,05
0,04
0,03
0,02
Abs
0
200
400
600
800
1000
Time (min)

- **pH 4.99**

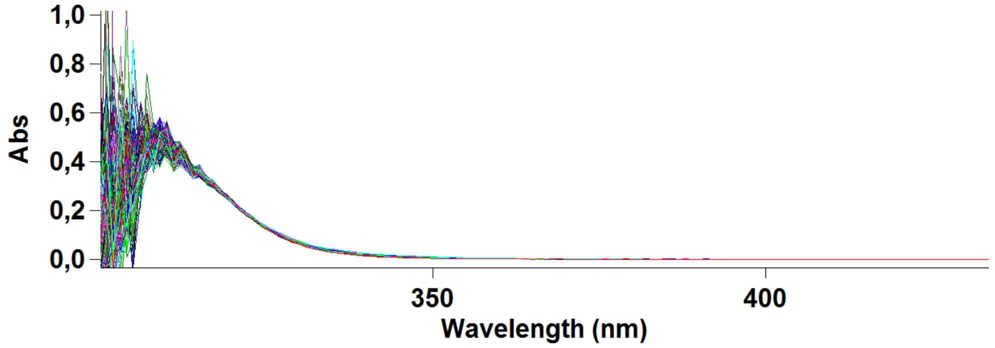
1,0
0,8
0,6
0,4
0,2
0,0
Abs
350
400
Wavelength (nm)

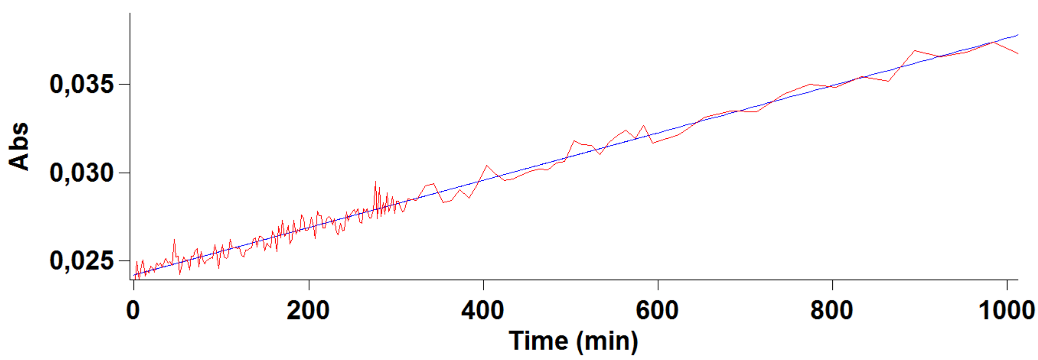
0,035
0,030
0,025
Abs
0
200
400
600
800
1000
Time (min)

- **pH 5.68**

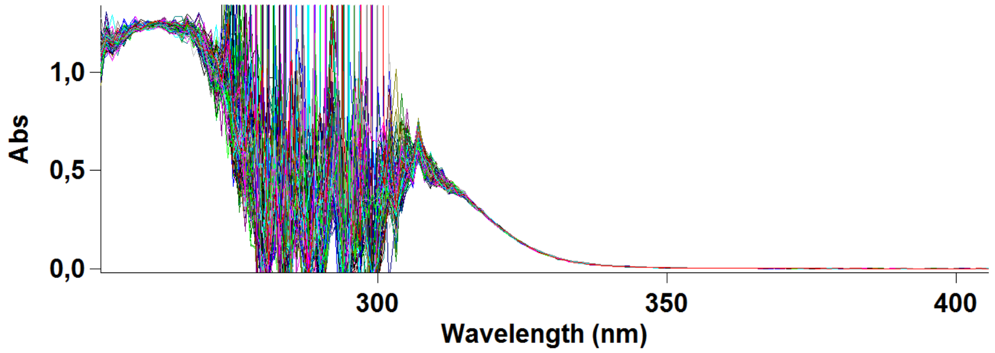
1,0
0,5
0,0
Abs
300
350
400
Wavelength (nm)

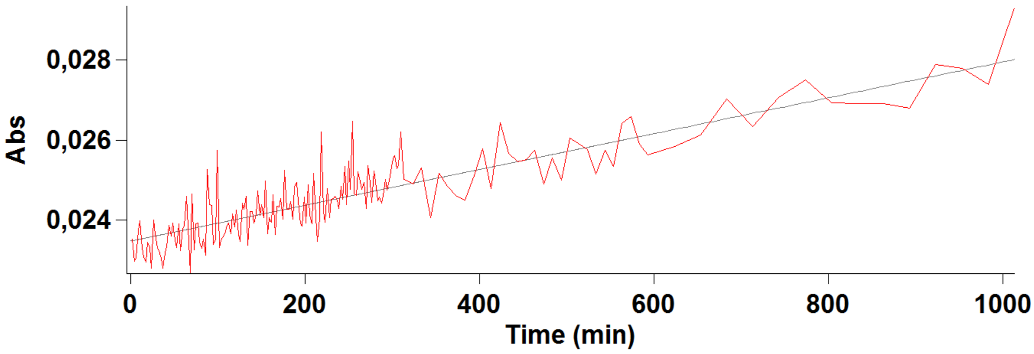
0,028
0,026
0,024
Abs
0
200
400
600
800
1000
Time (min)

- **pH 6.40**

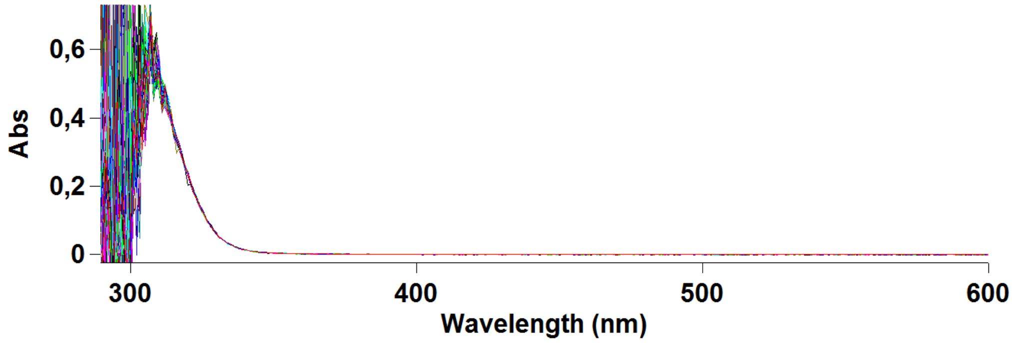
0,6
0,4
0,2
0
Abs
300
400
500
600
Wavelength (nm)

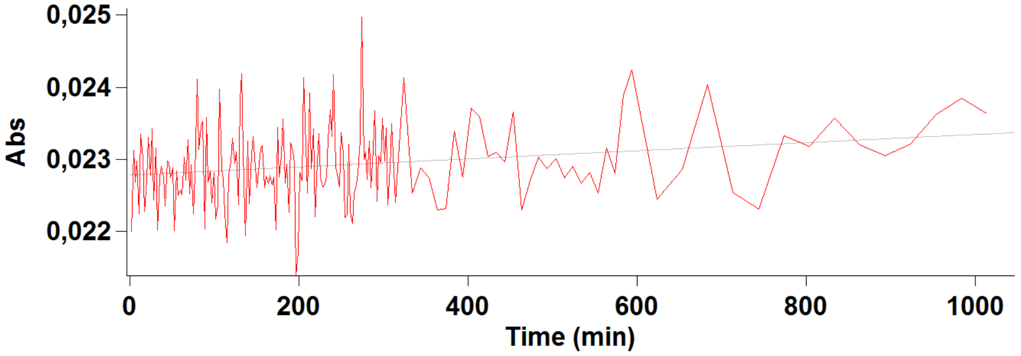
0,025
0,024
0,023
0,022
Abs
0
200
400
600
800
1000
Time (min)

Influence of P5A concentration on CPA decomposition at different pHs

pH 2.50

[P5A] = 0 M

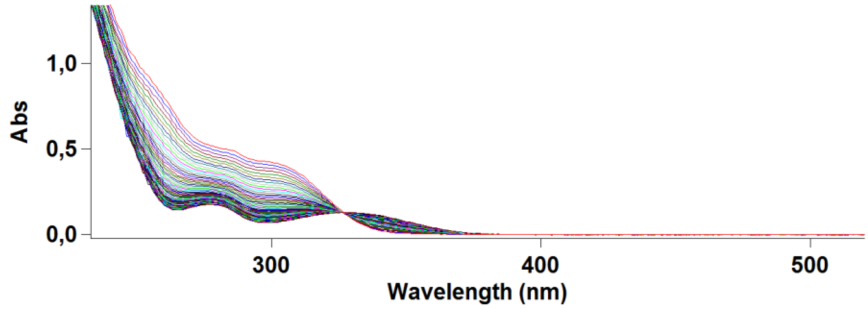

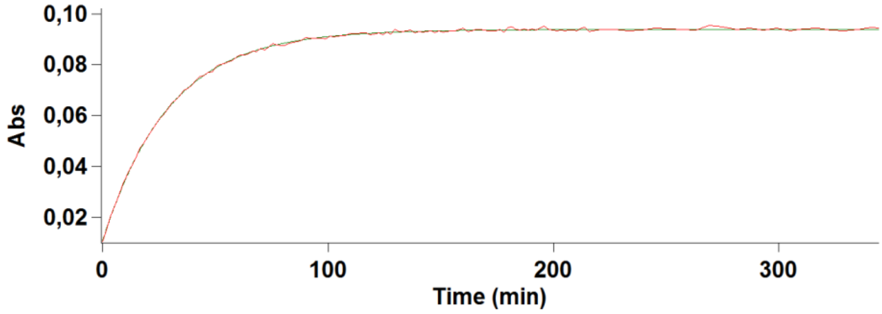

[P5A] = 1.20 x 10^{-6} M

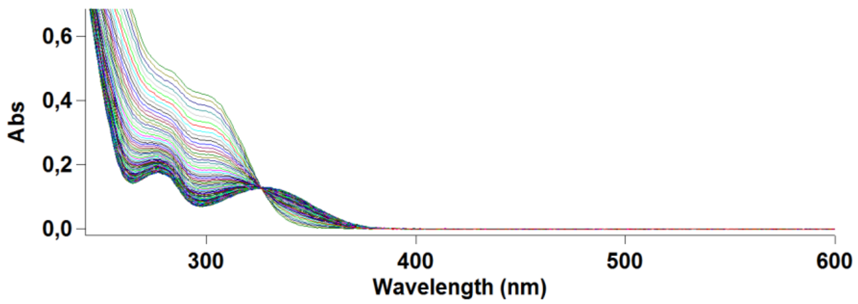

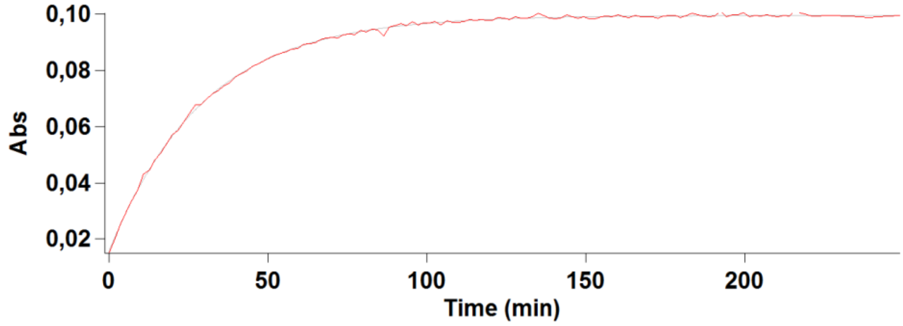

[P5A] = 4.00 x 10^{-6} M

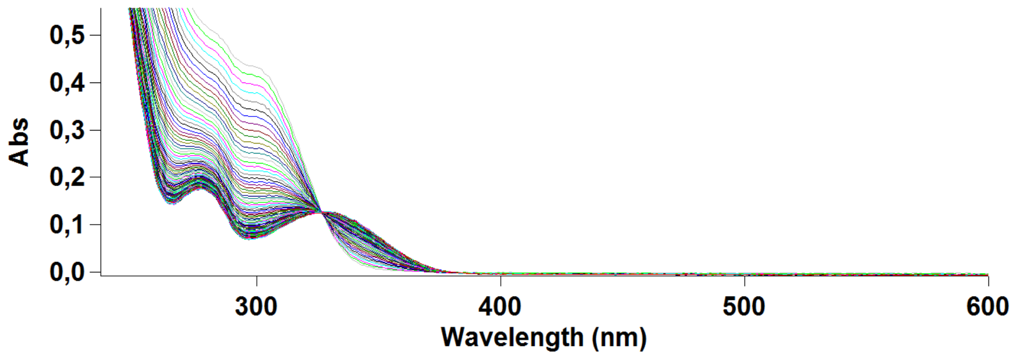

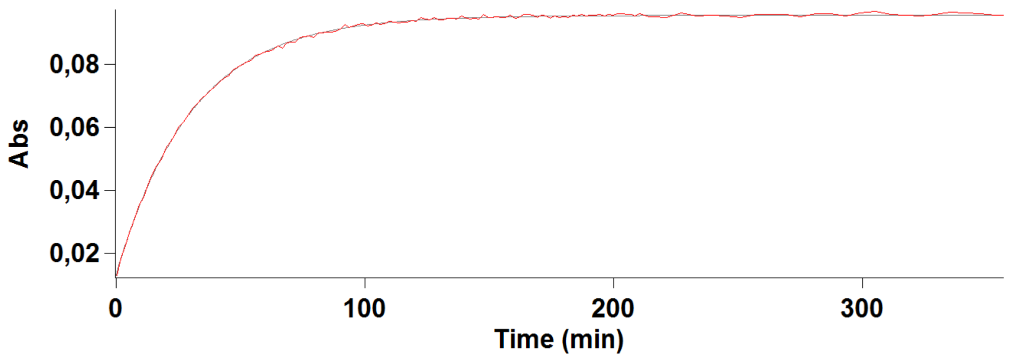

[P5A] = 6.00 x 10^{-6} M

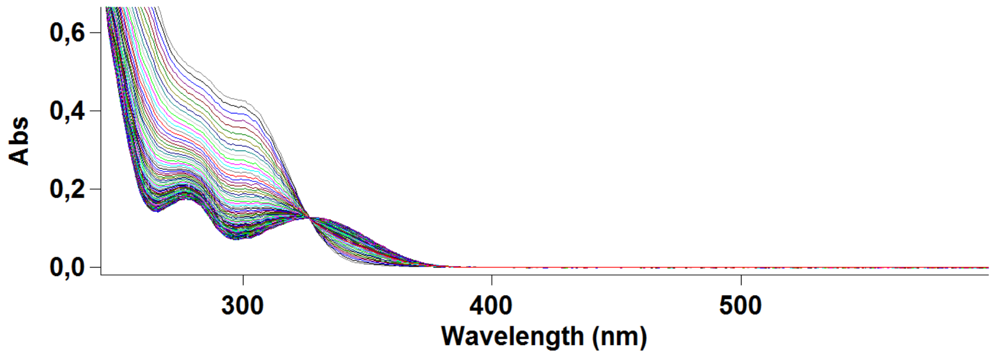

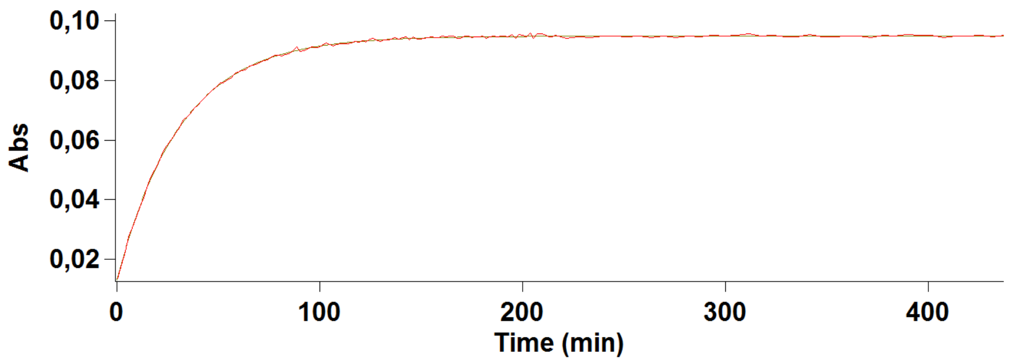

[P5A] = 8.00 x 10^{-6} M

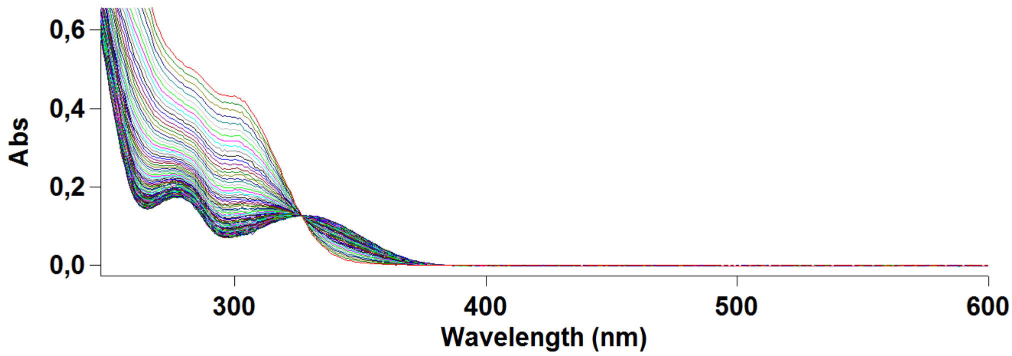

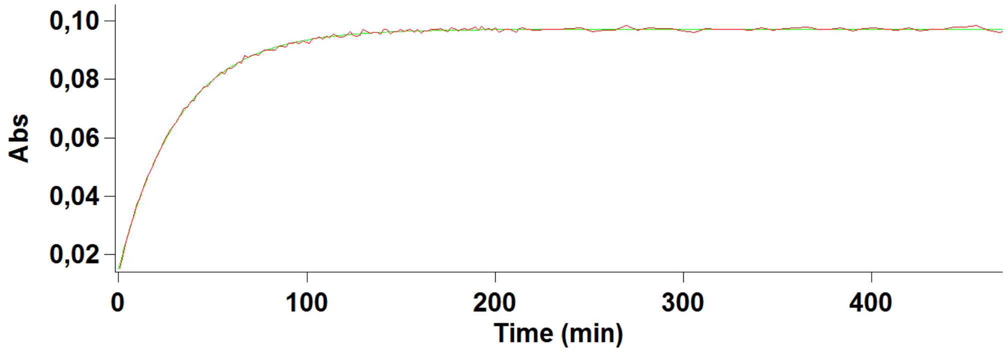

[P5A] = 1.00 x 10^{-5} M

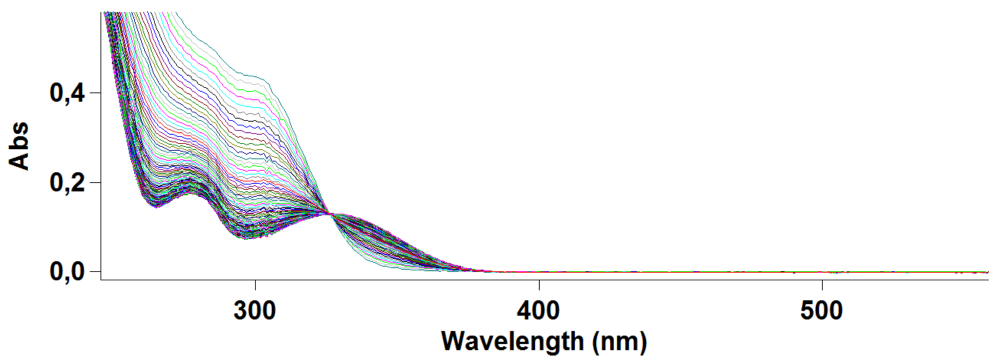

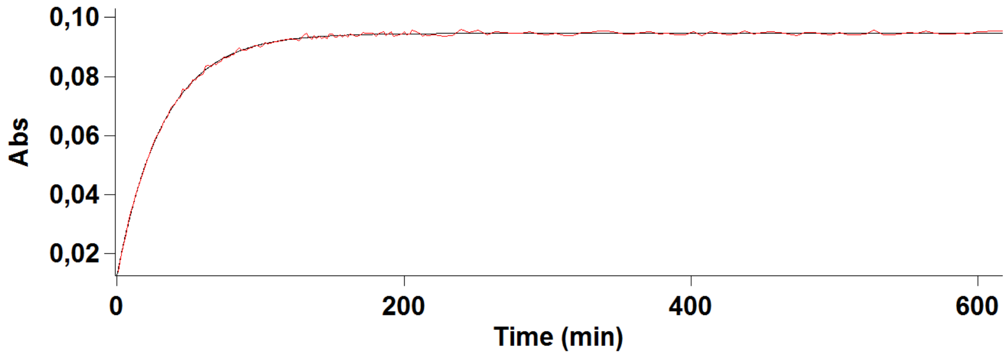

[P5A] = 3.00 x 10^{-5} M

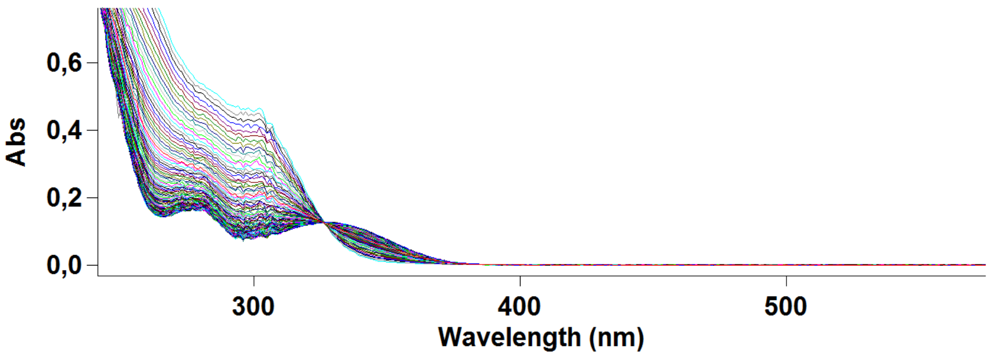

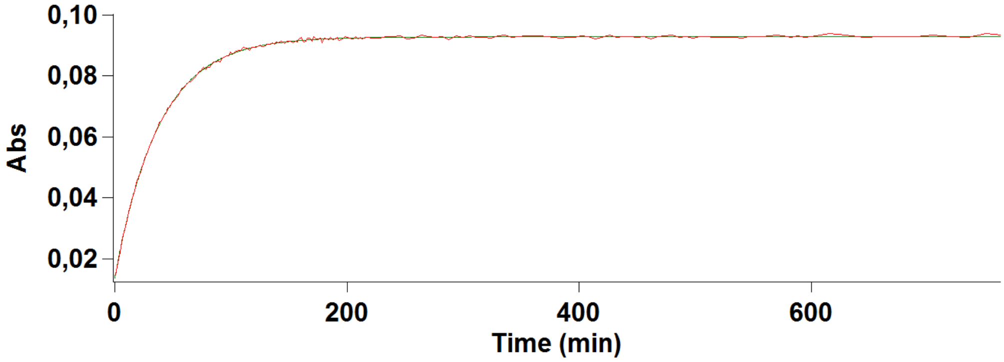

[P5A] = 5.00 x 10^{-5} M

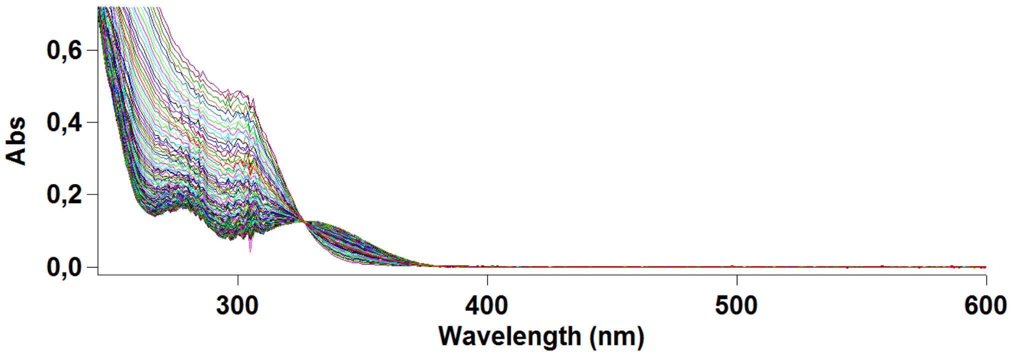

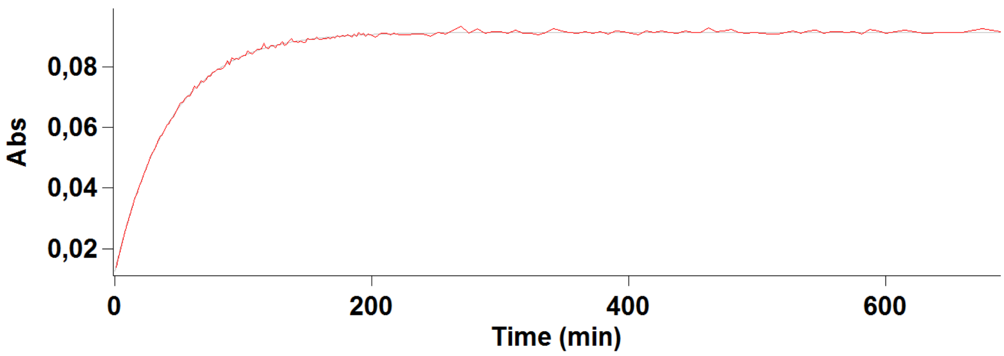

[P5A] = 8.00 x 10^{-5} M

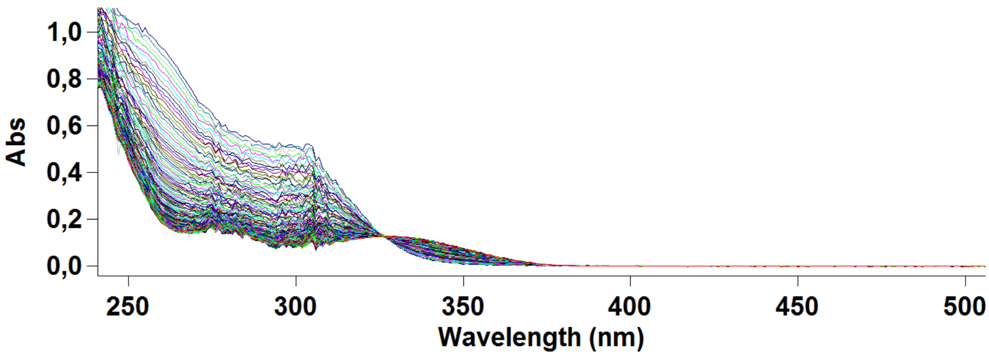

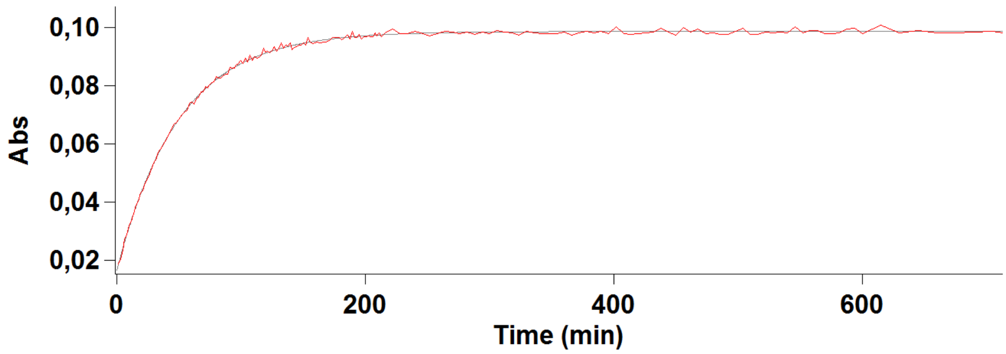

[P5A] = 1.00 x 10^{-4} M

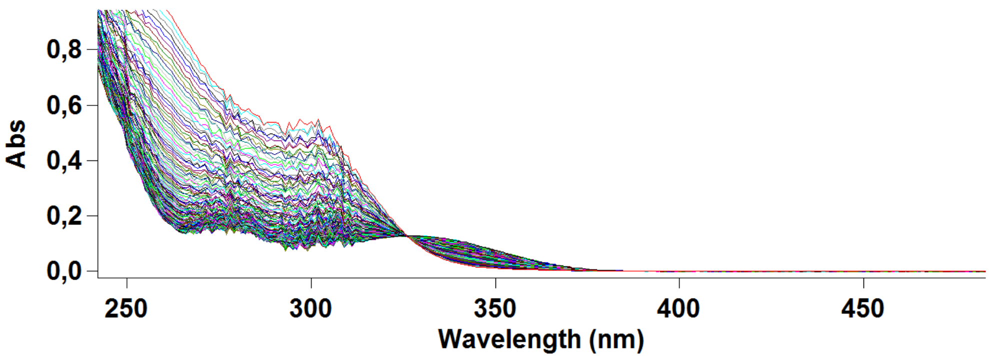

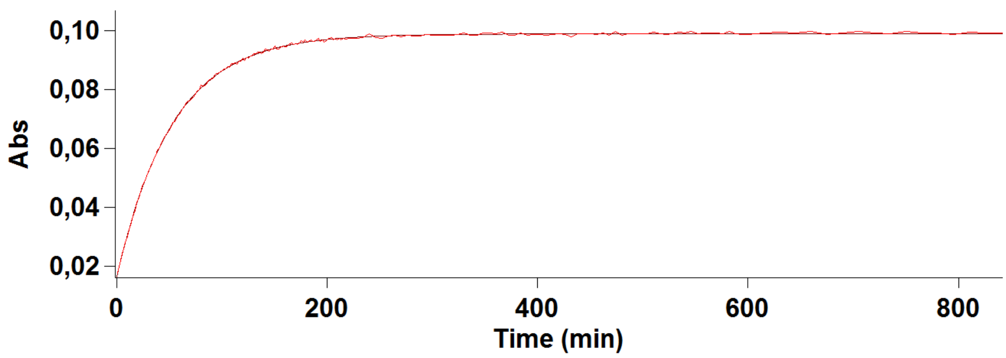

[P5A] = 3.00 x 10^{-4} M

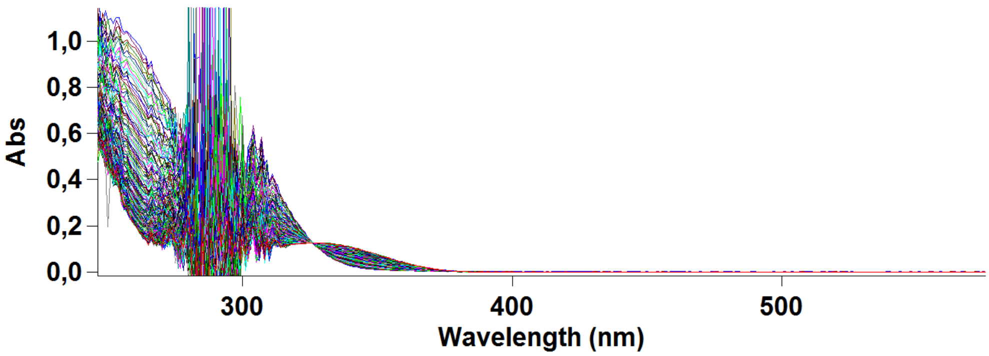

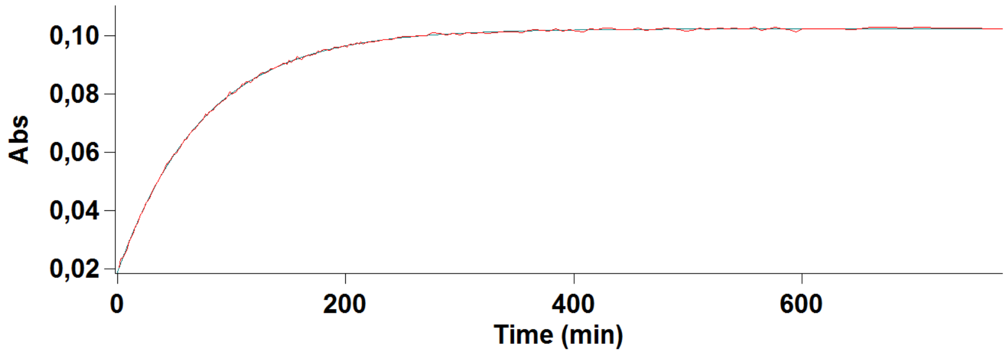

[P5A] = 5.00 x 10^{-4} M

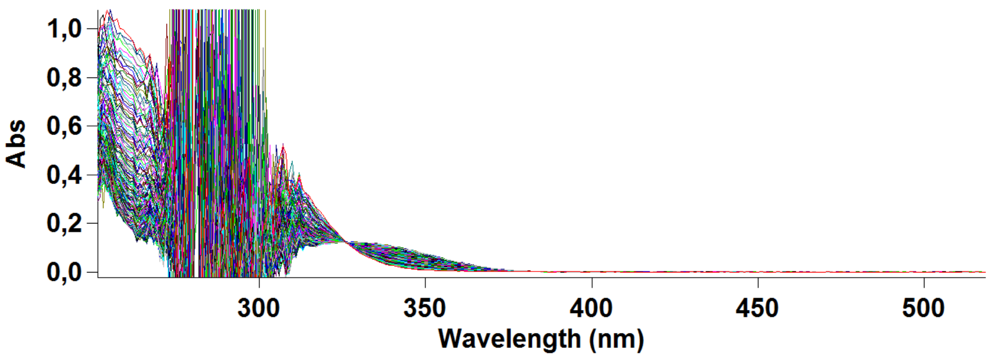

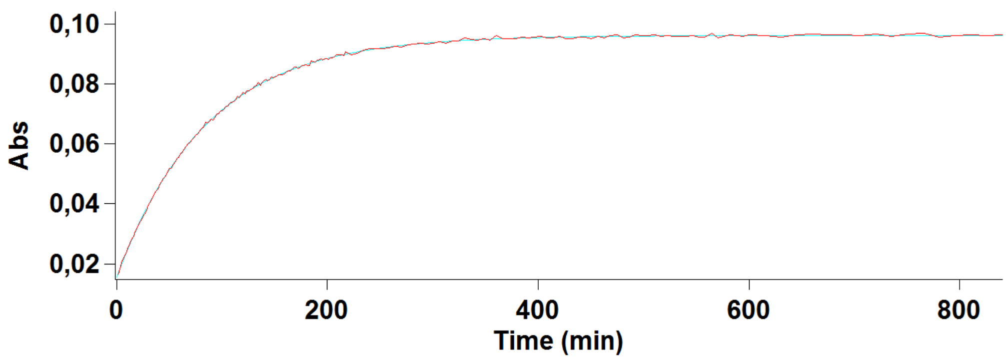

[P5A] = 8.00 x 10^{-4} M

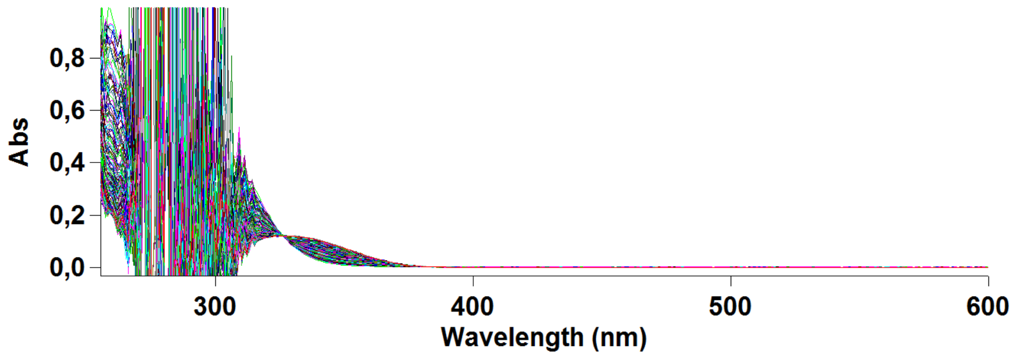

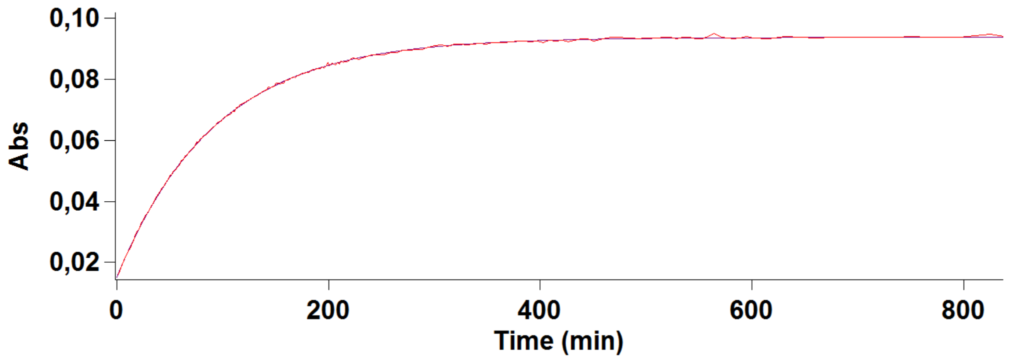

[P5A] = 2.00 x 10^{-3} M

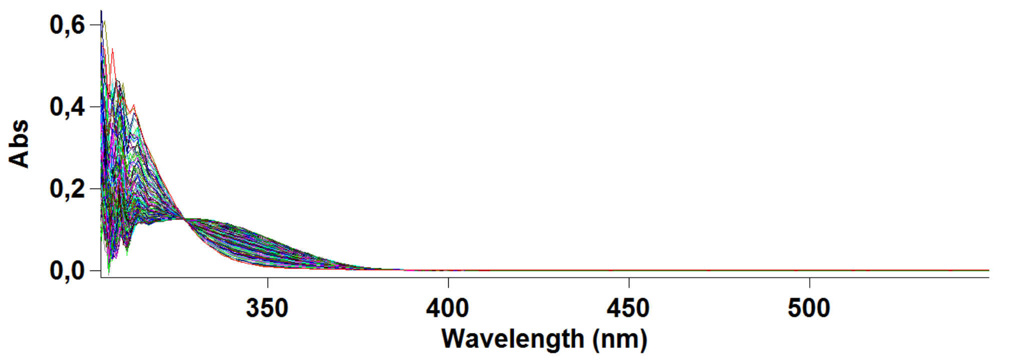

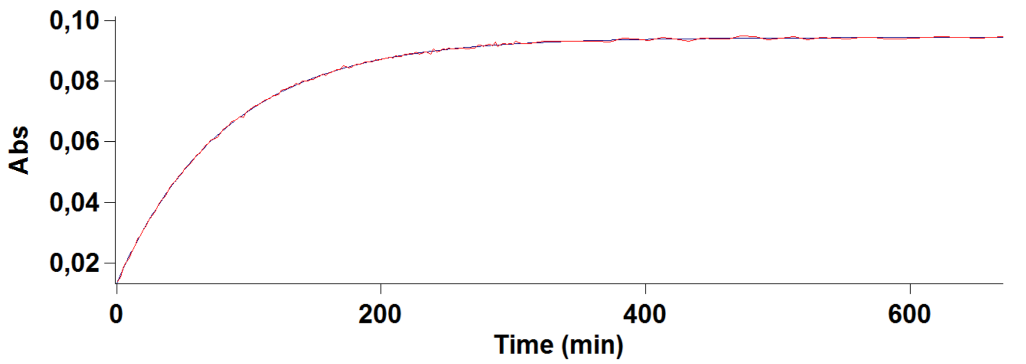

pH 3.45

[P5A] = 0 M

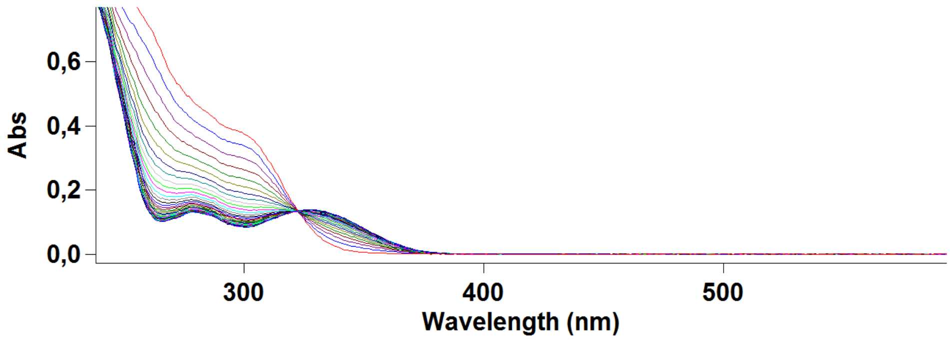

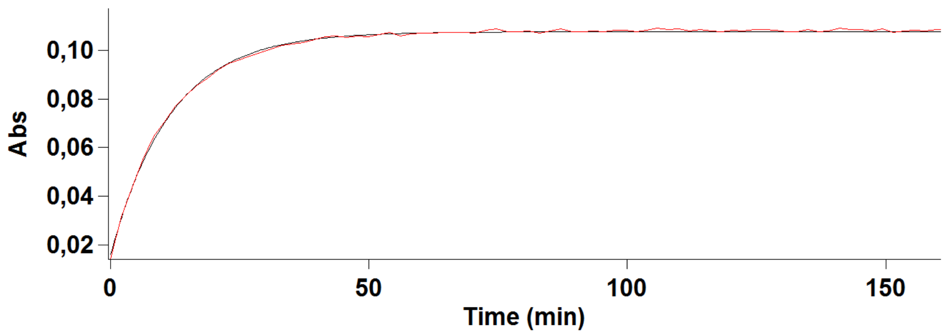

[P5A] = 1.20 x 10^{-6} M

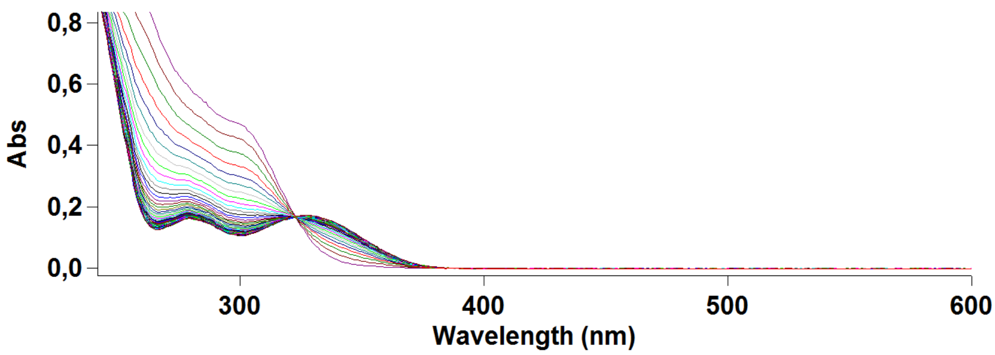

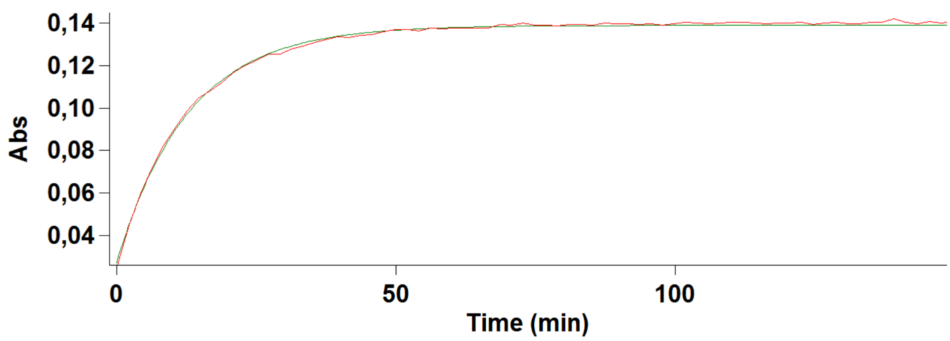

[P5A] = 4.00 x 10^{-6} M

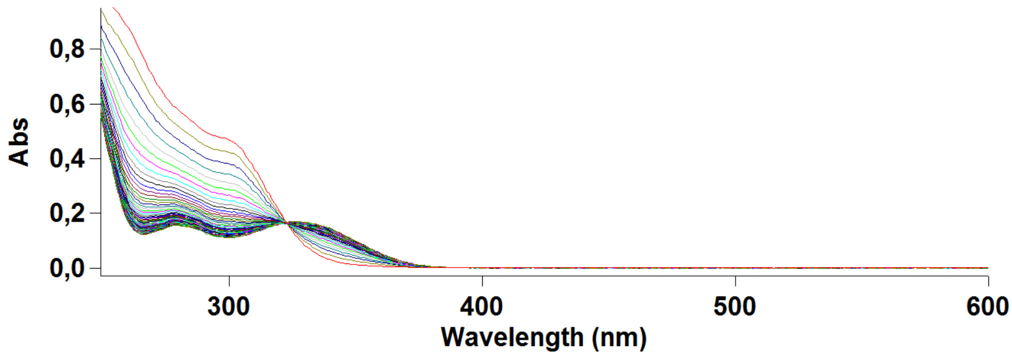

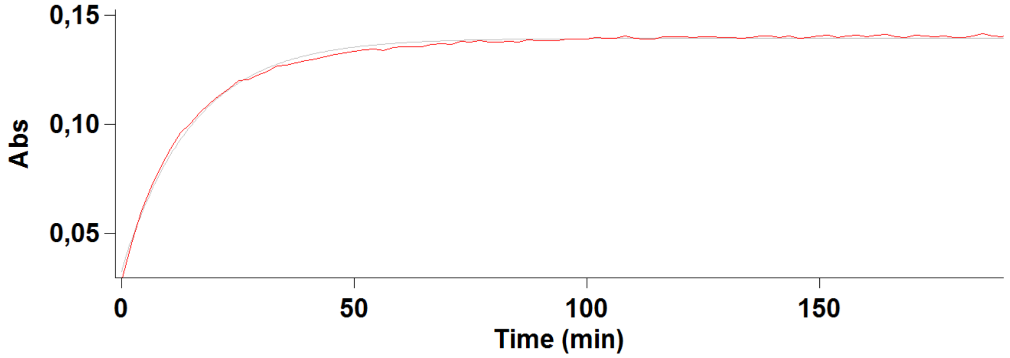

[P5A] = 6.00 x 10^{-6} M

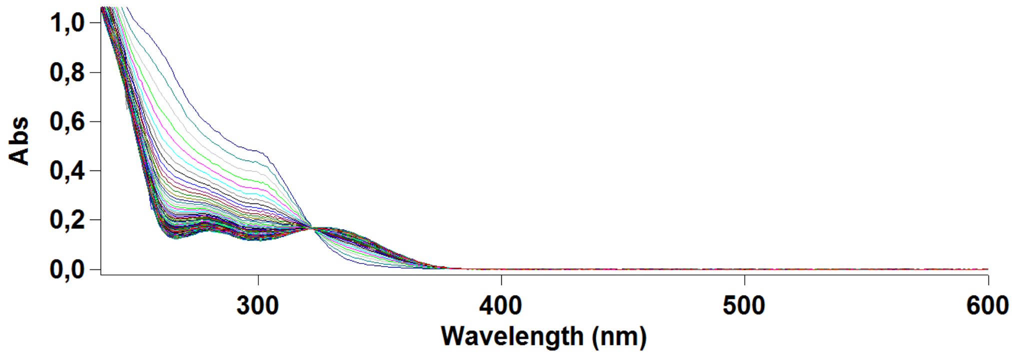

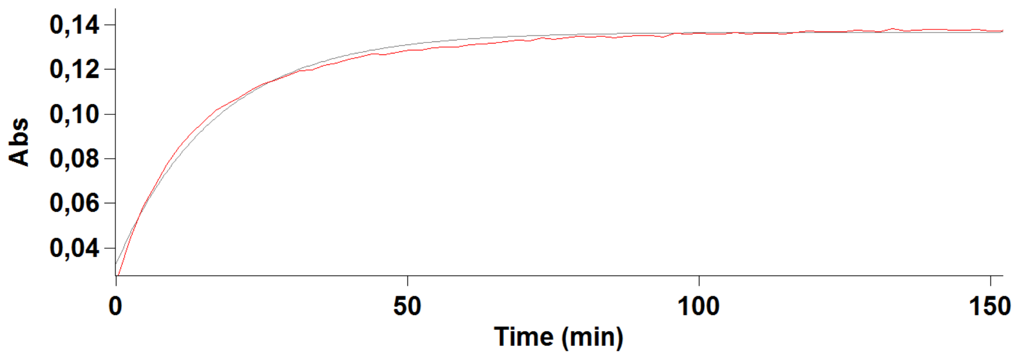

[P5A] = 8.00 x 10^{-6} M

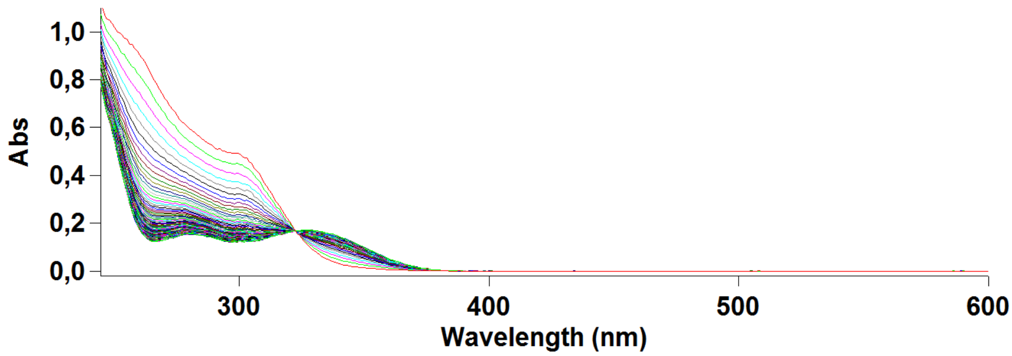

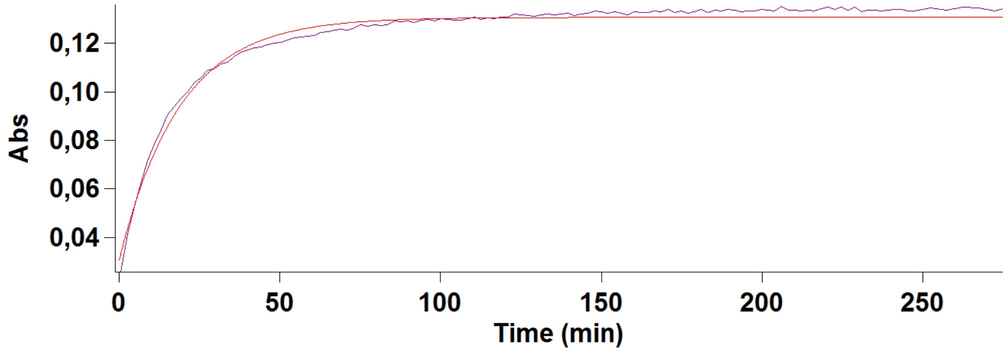

[P5A] = 1.00 x 10^{-5} M

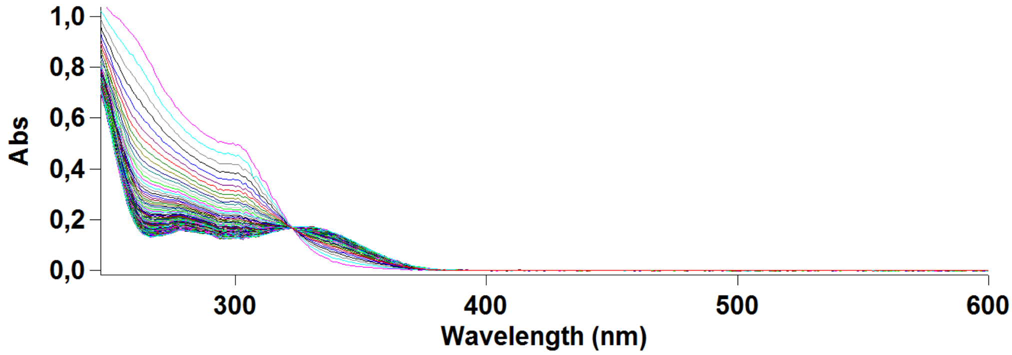

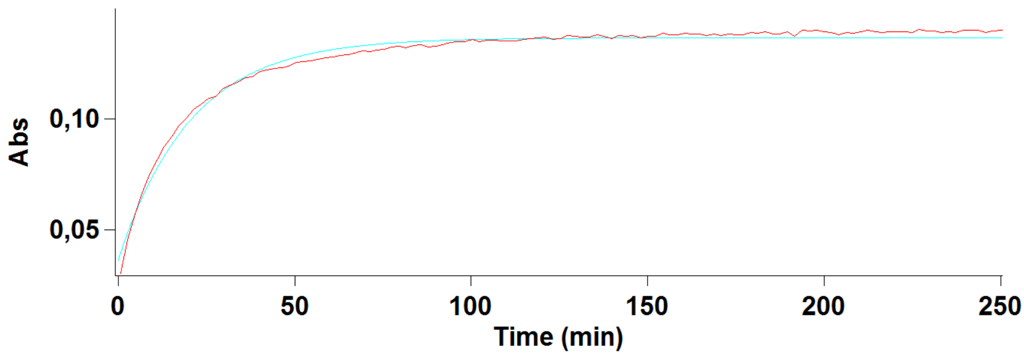

For concentrations greater than 3.00×10^{-5} M, the absorbance changes presented a gradually different behavior from a typical first-order profile. This is probably due to a competition between CPA and one or both fragments of its decomposition for the P5A cavity. Thus, the k_{obs} were calculated by the initial velocity method.

[P5A] = 3.00 x 10^{-5} M

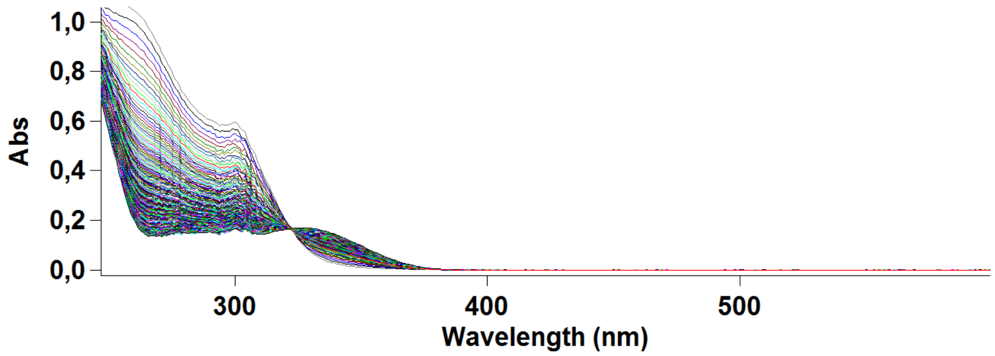

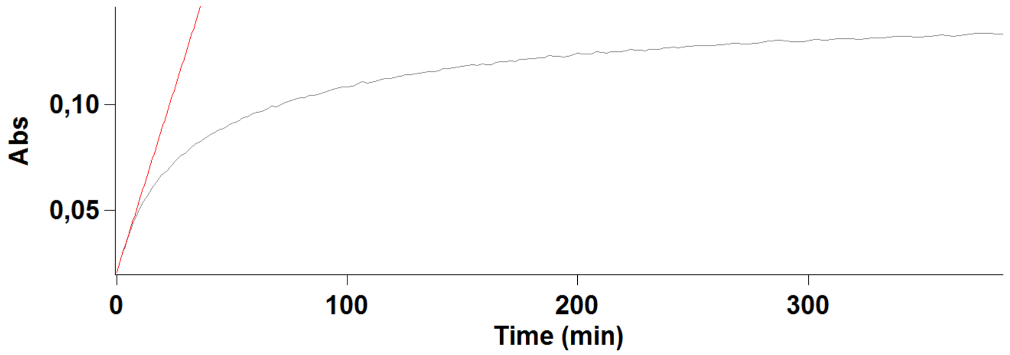

[P5A] = 5.00 x 10^{-5} M

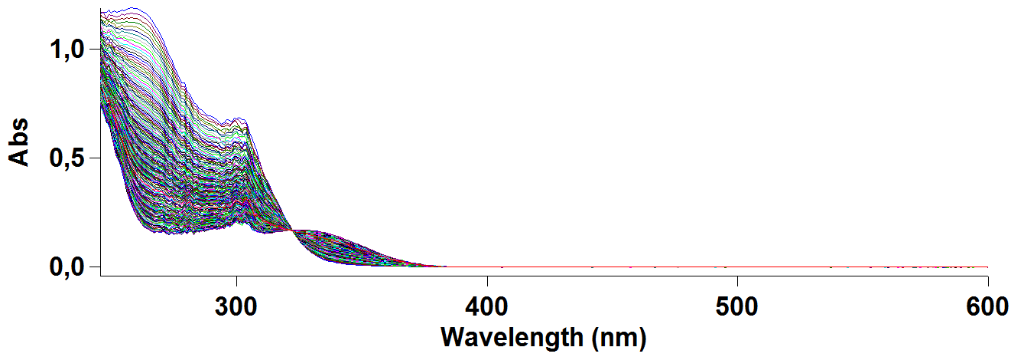

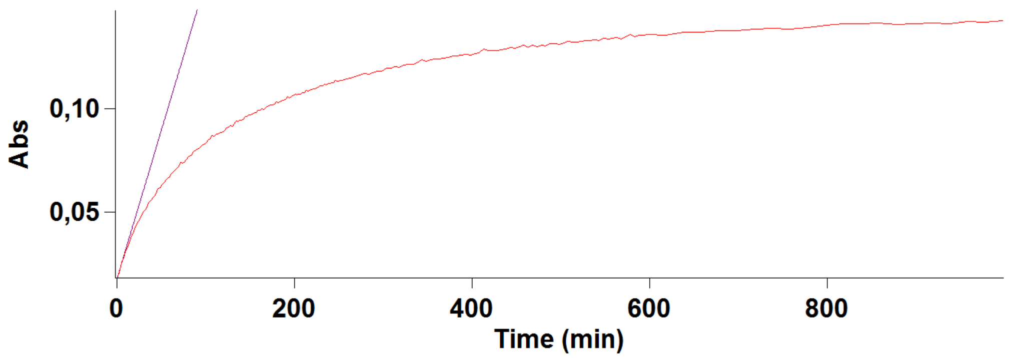

[P5A] = 8.00 x 10^{-5} M

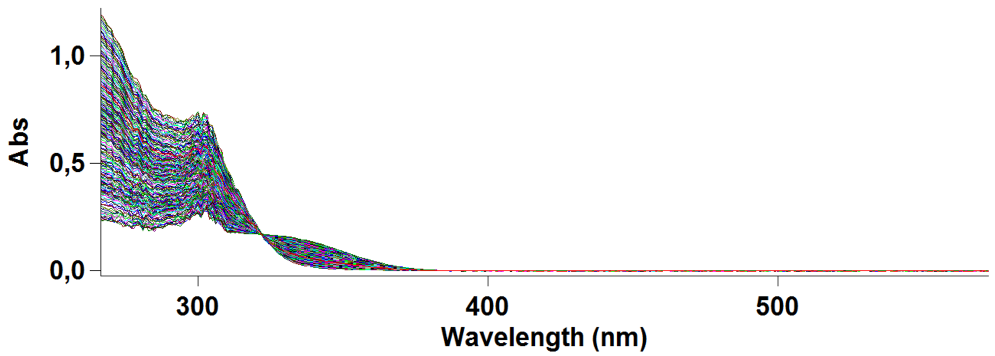

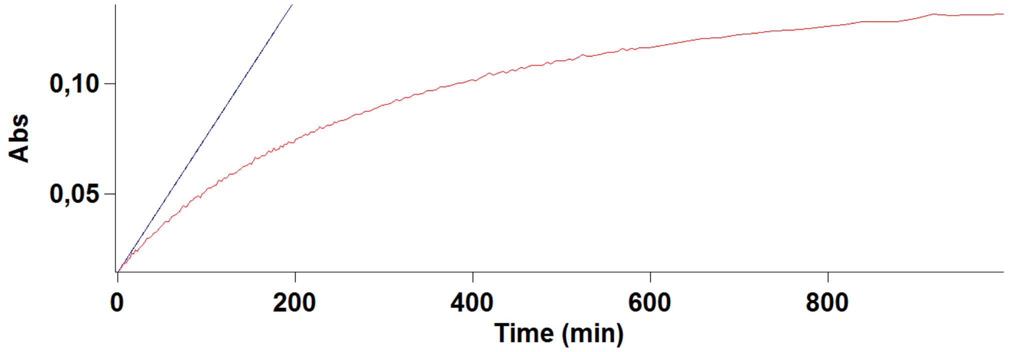

[P5A] = 1.00 x 10^{-4} M

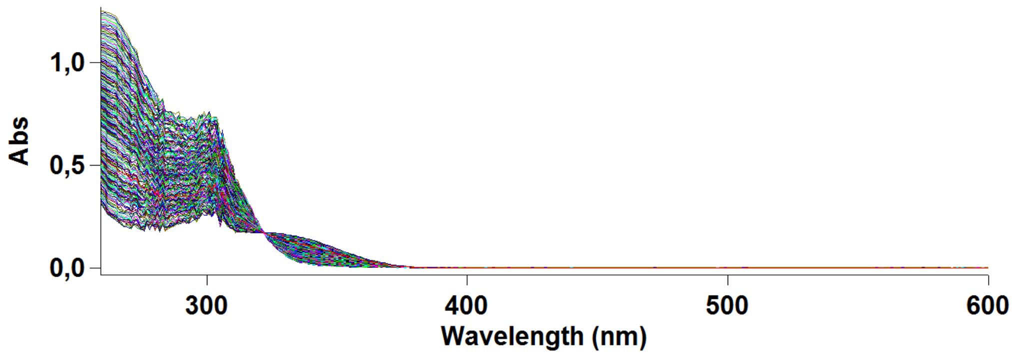

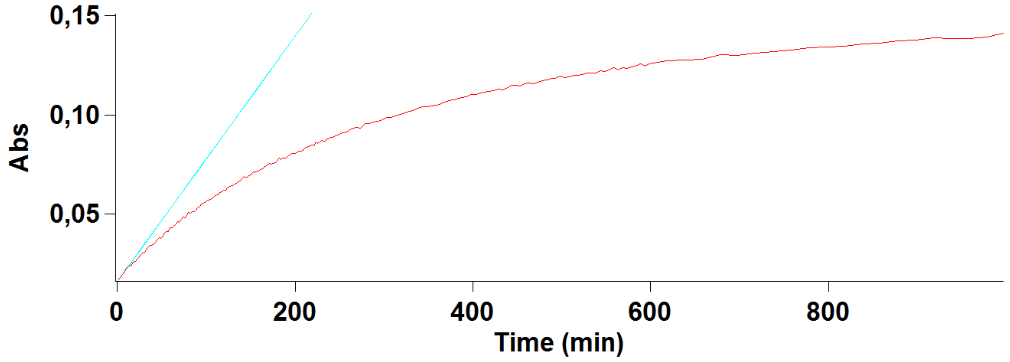

[P5A] = 3.00 x 10^{-4} M

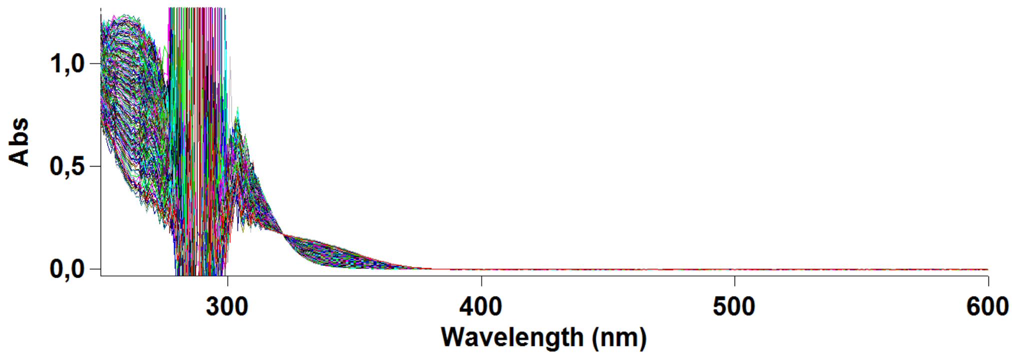

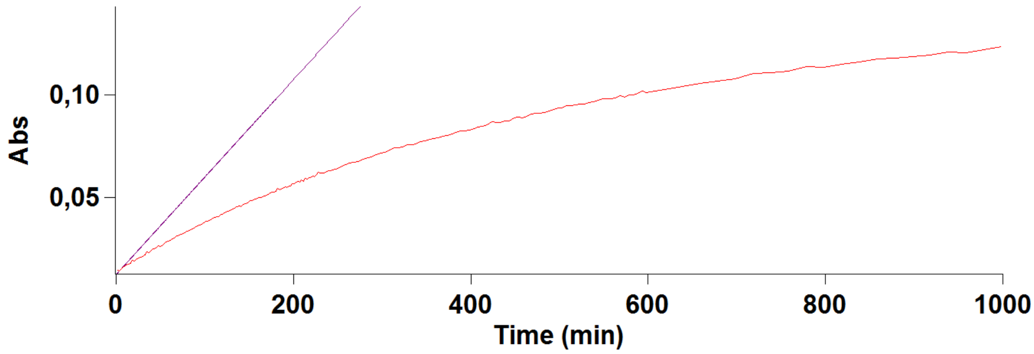

[P5A] = 8.00 x 10^{-4} M

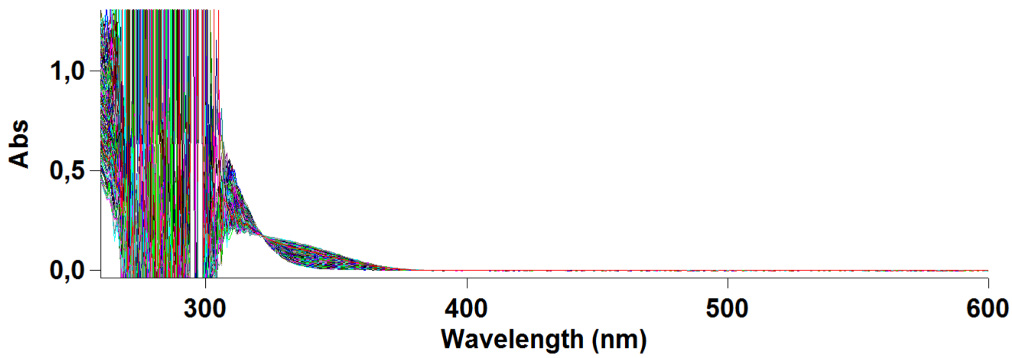

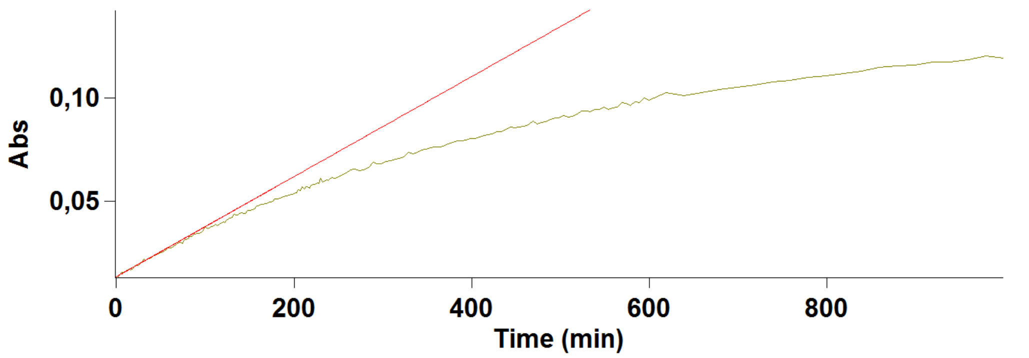

[P5A] = 2.00 x 10^{-3} M

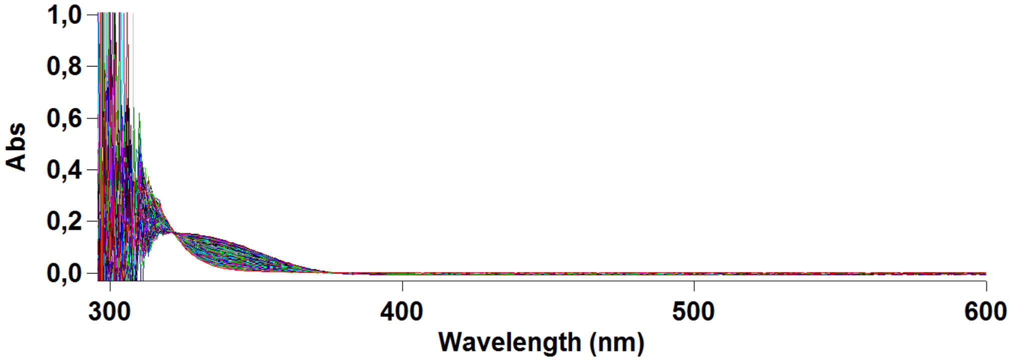

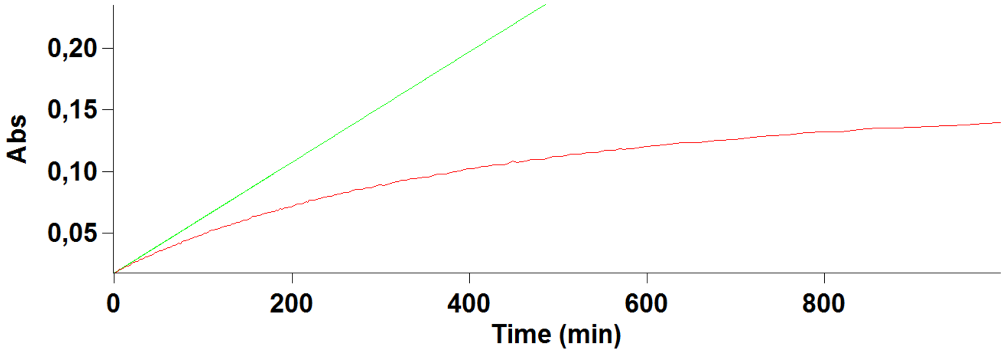

pH 4.25

[P5A] = 0 M

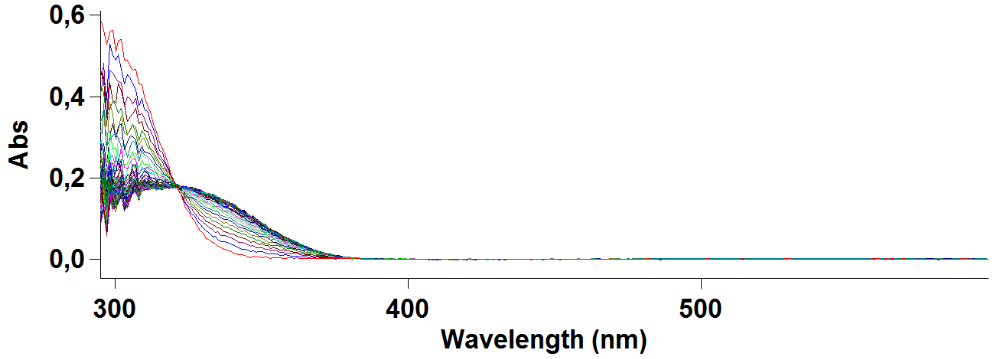

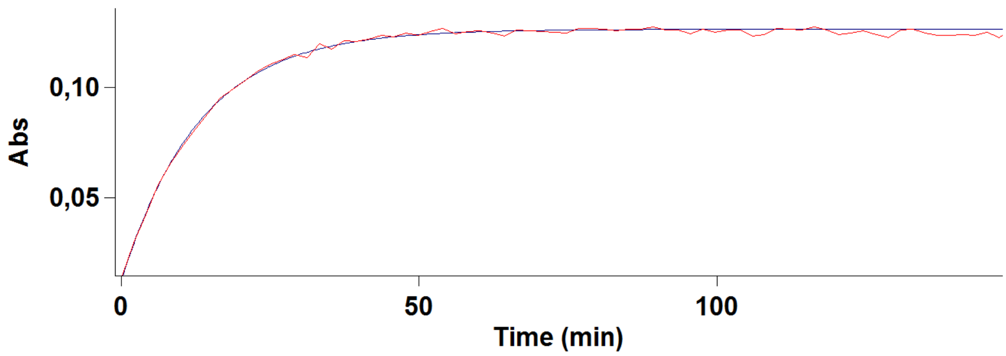

[P5A] = 1.20 x 10^{-6} M

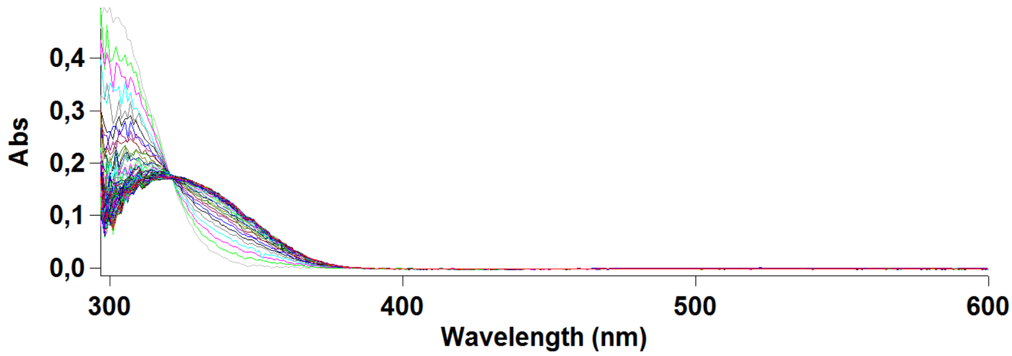

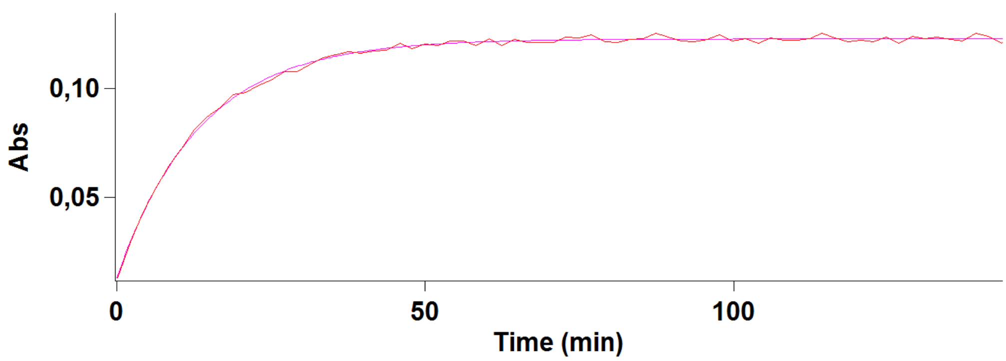

[P5A] = 4.00 x 10^{-6} M

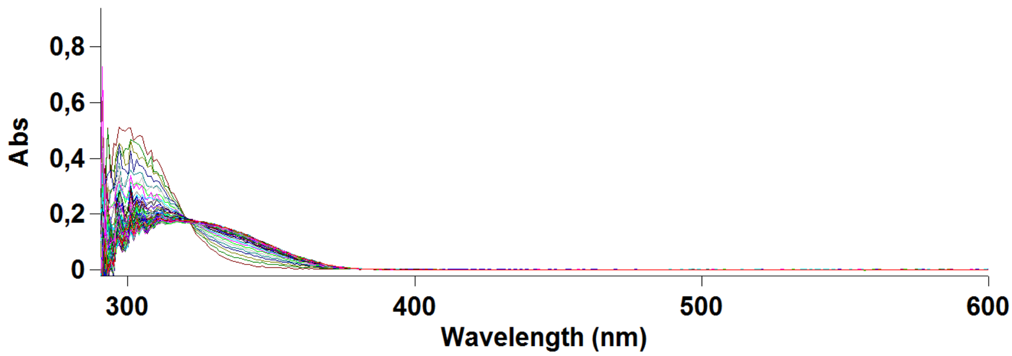

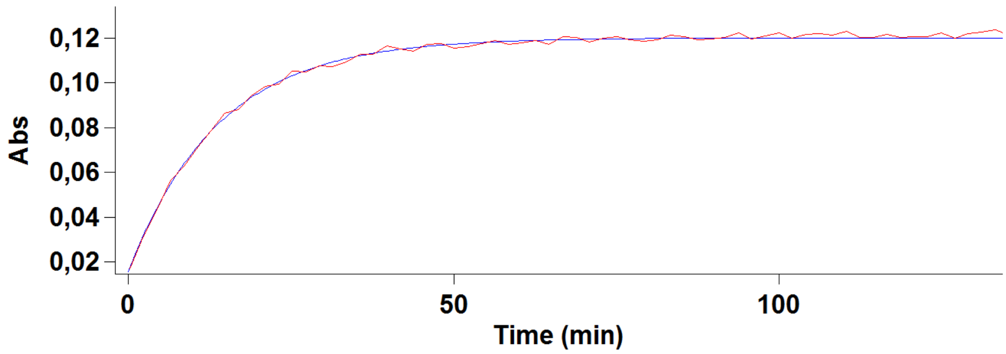

[P5A] = 8.00 x 10^{-6} M

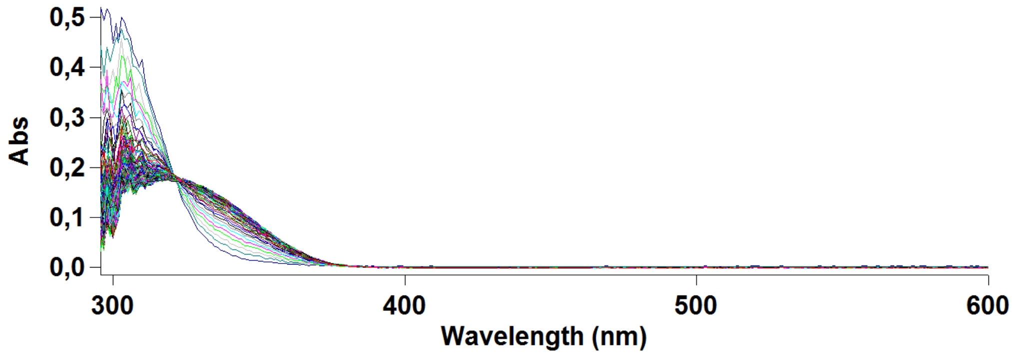

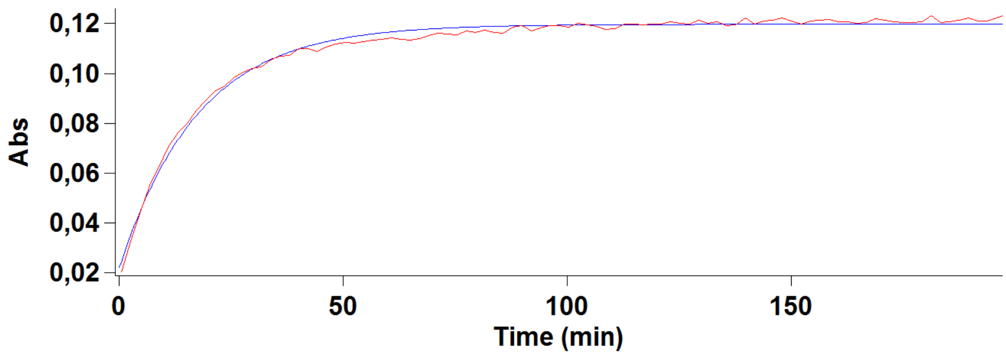

[P5A] = 3.00 x 10^{-5} M

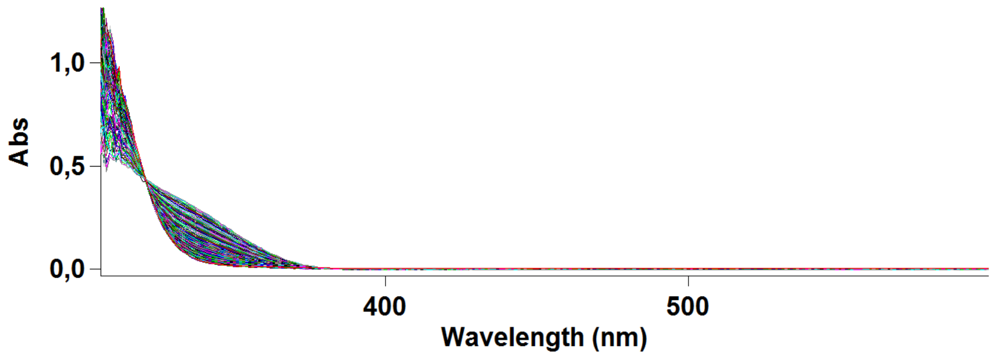

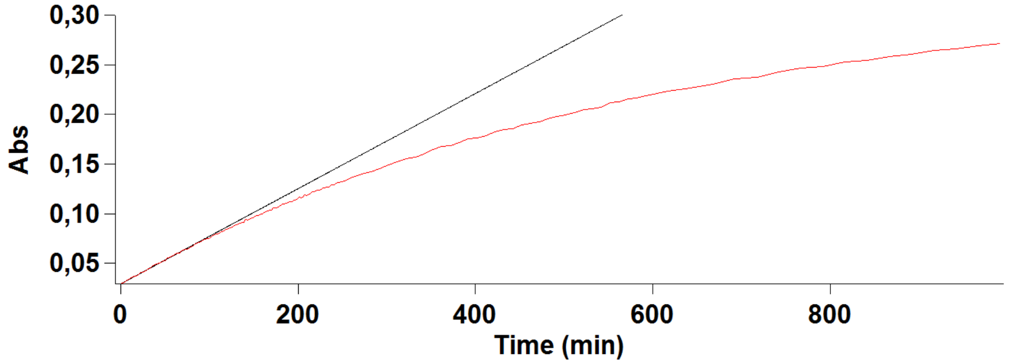

[P5A] = 5.00 x 10^{-5} M

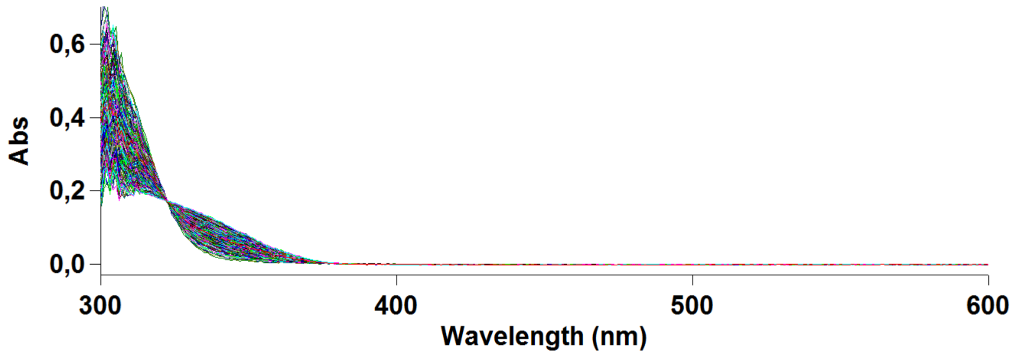

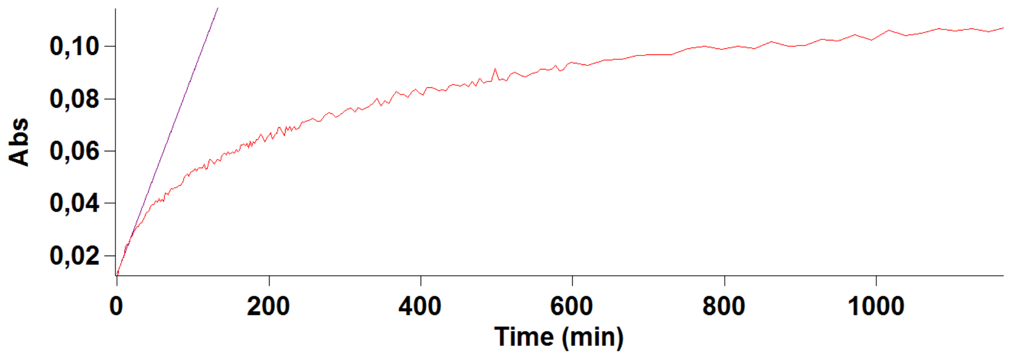

[P5A] = 8.00 x 10^{-5} M

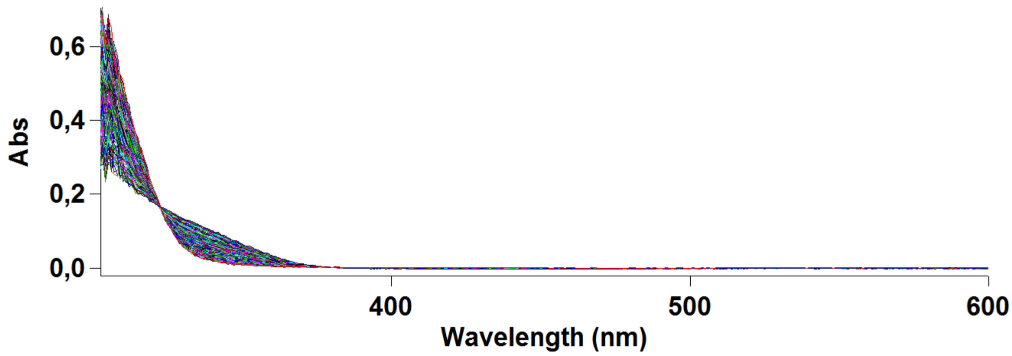

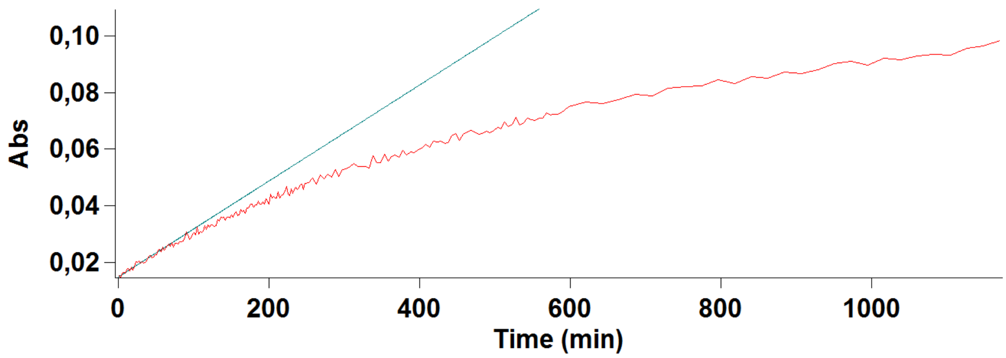

[P5A] = 1.00 x 10^{-4} M

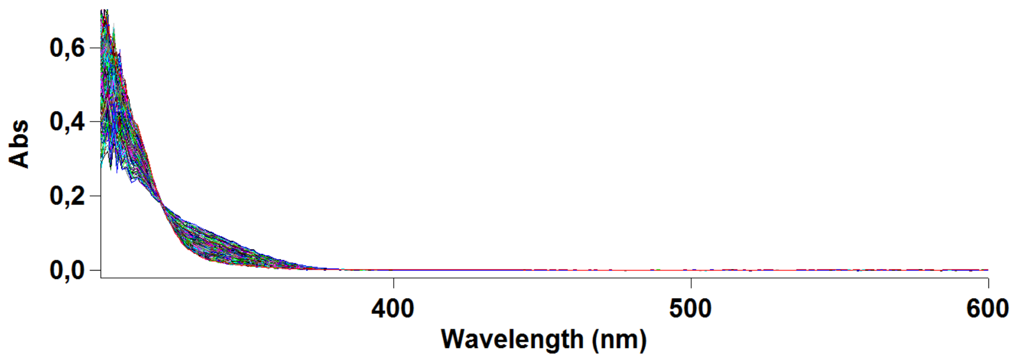

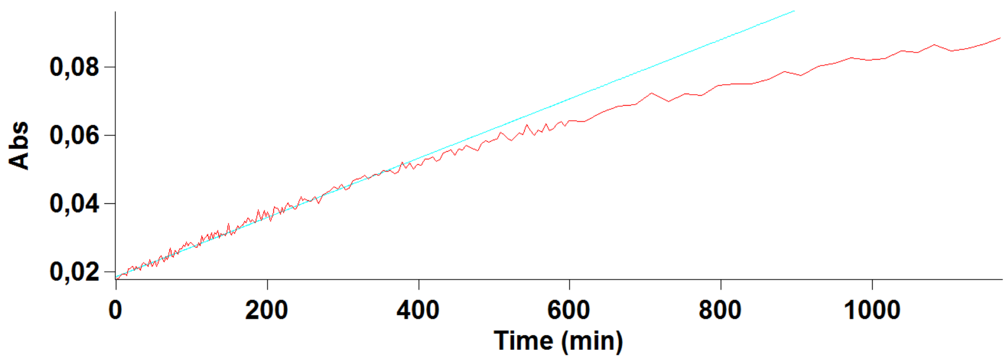

[P5A] = 3.00 x 10^{-4} M

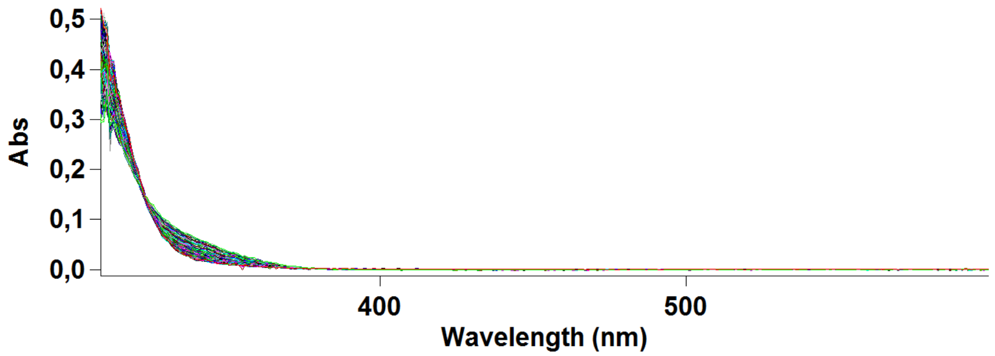

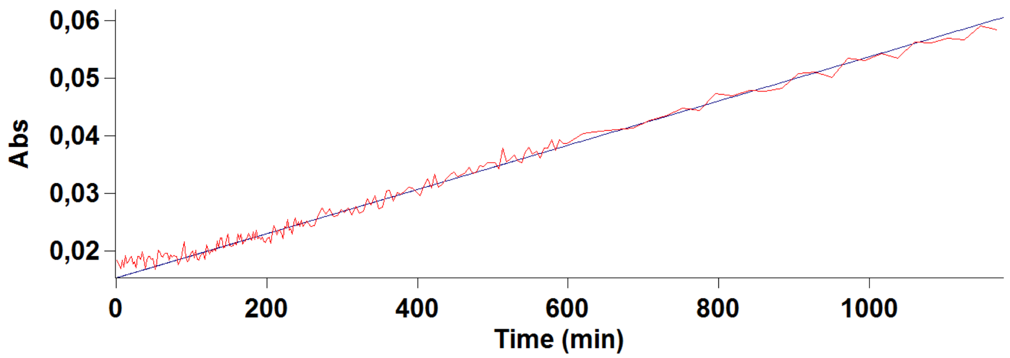

[P5A] = 8.00 x 10^{-4} M

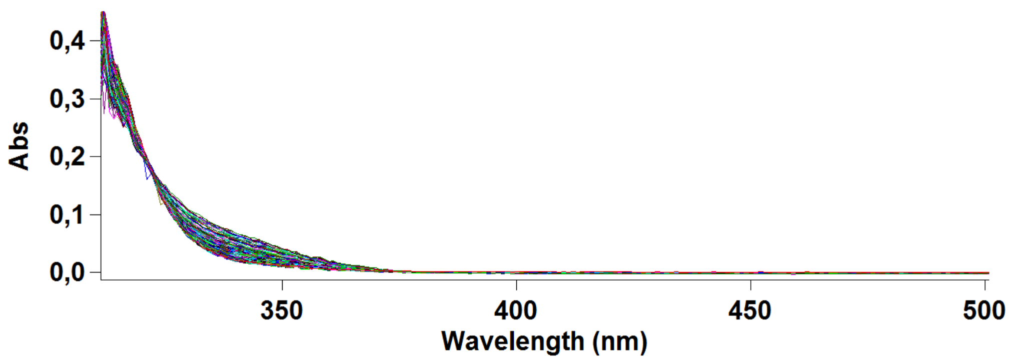

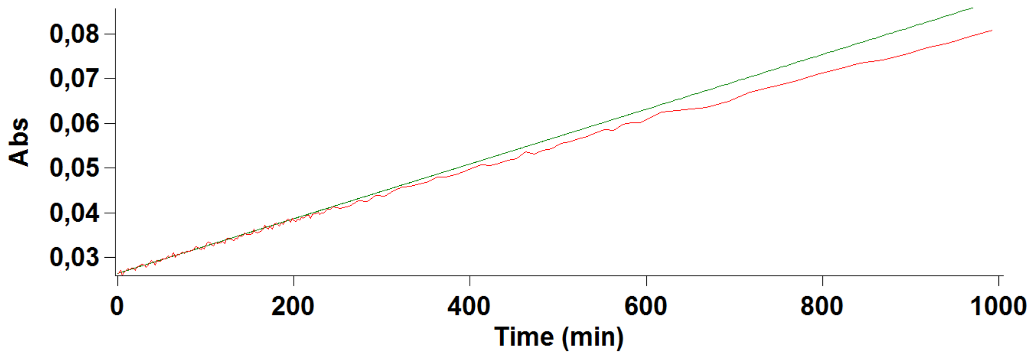

[P5A] = 2.00 x 10^{-3} M

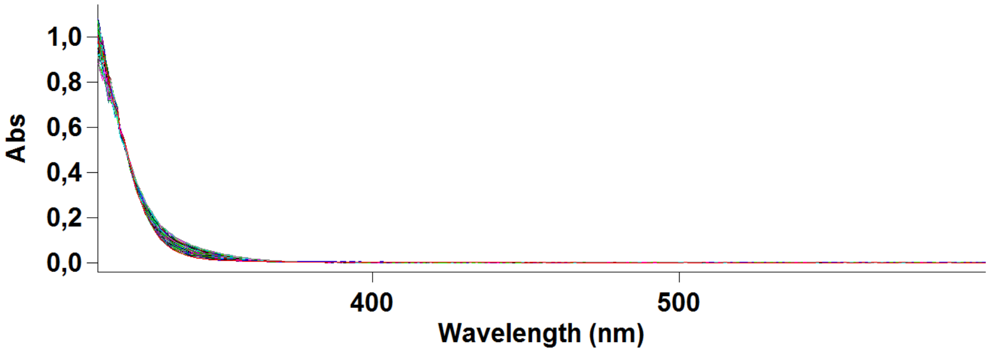

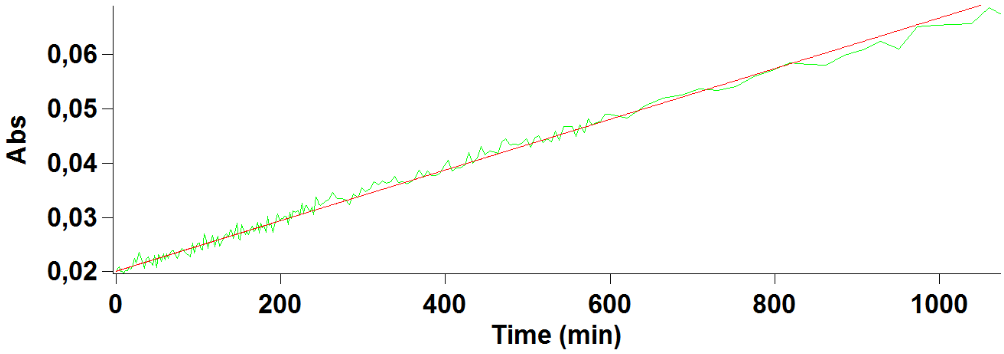

pH 6.00

[P5A] = 0 M

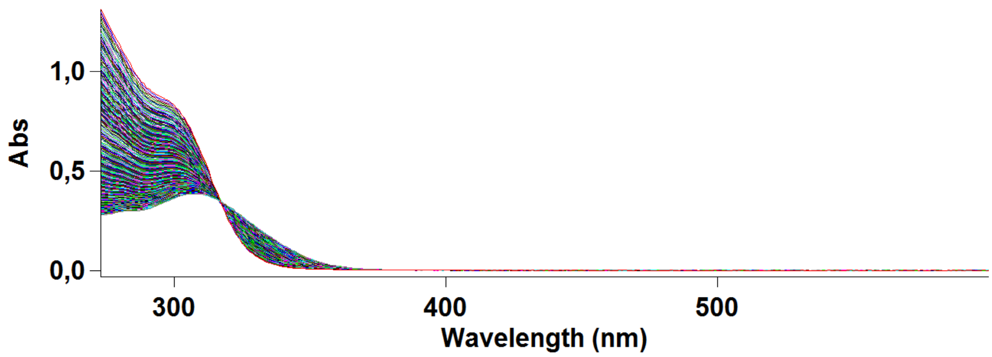

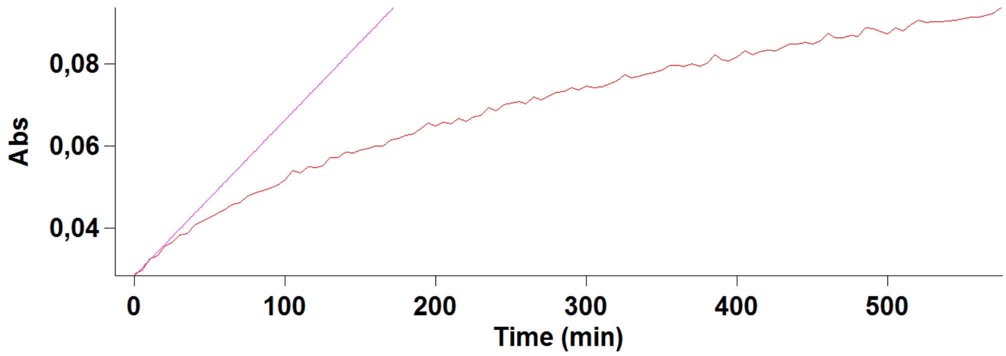

[P5A] = 2.00 x 10^{-6} M

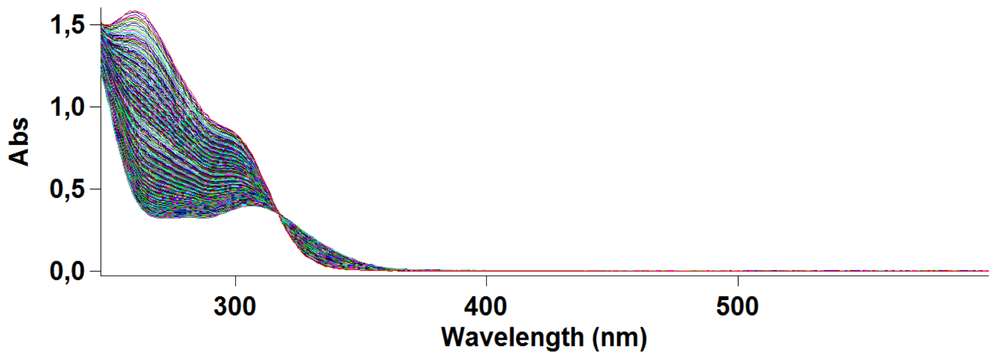

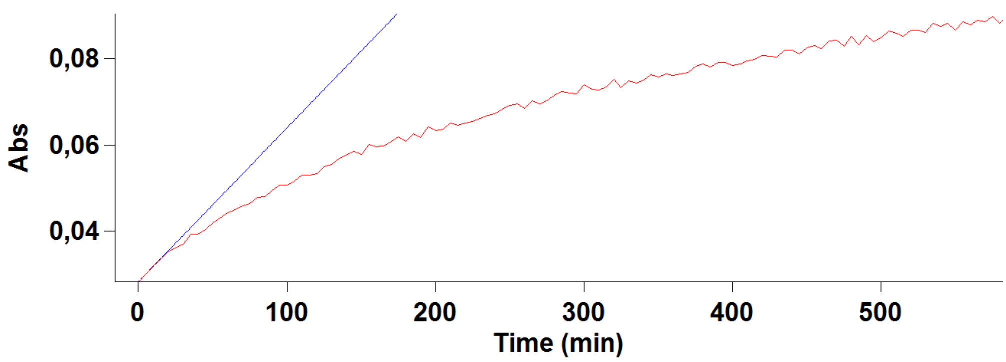

[P5A] = 6.00 x 10^{-6} M

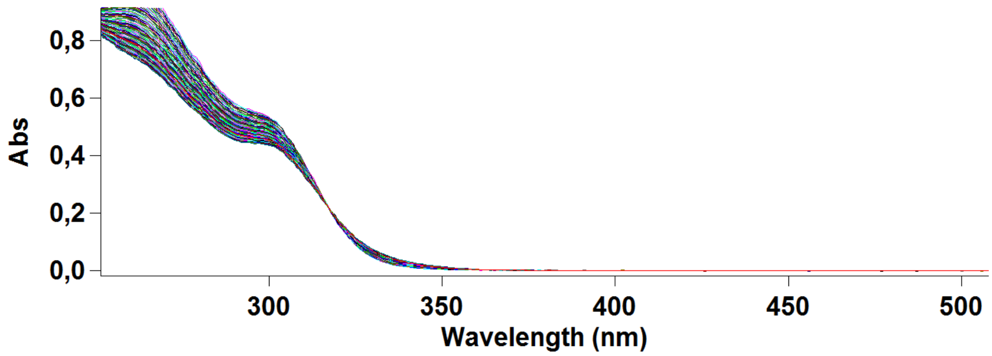

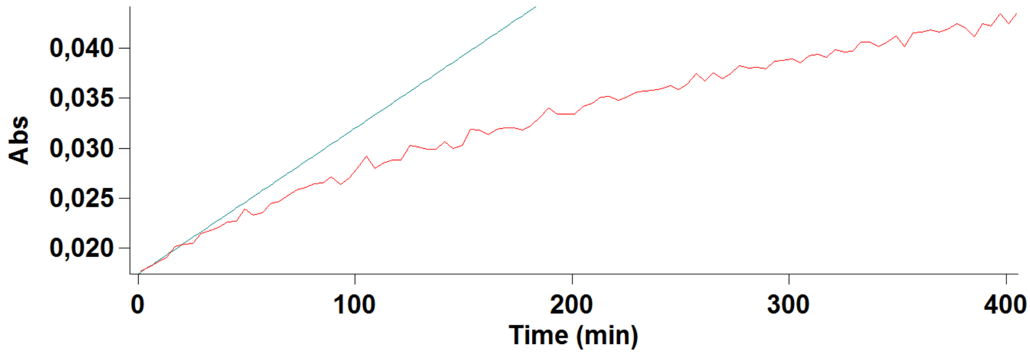

[P5A] = 2.00 x 10^{-5} M

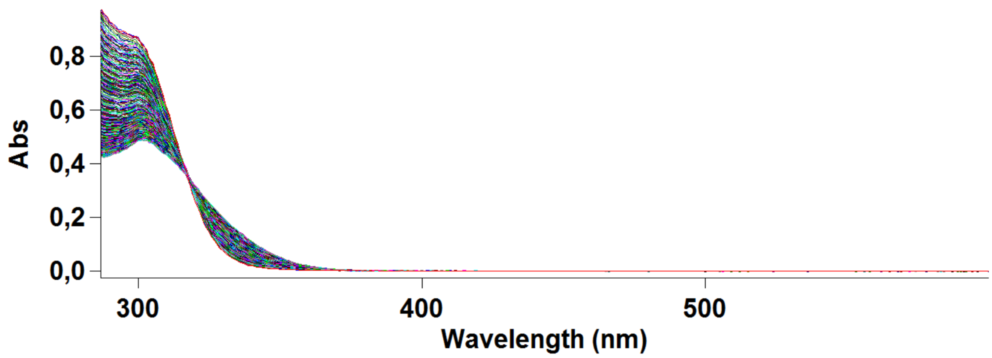

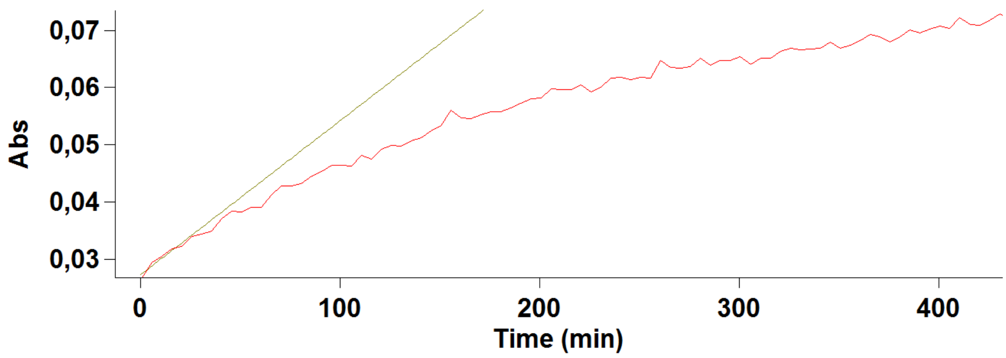

[P5A] = 4.00 x 10^{-5} M

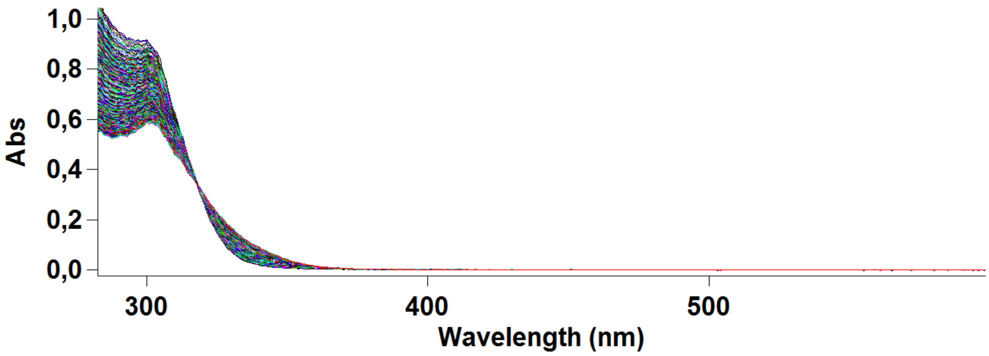

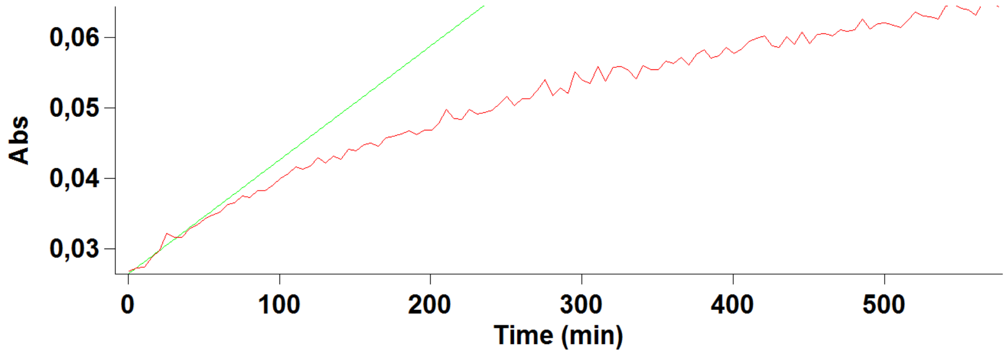

[P5A] = 8.00 x 10^{-5} M

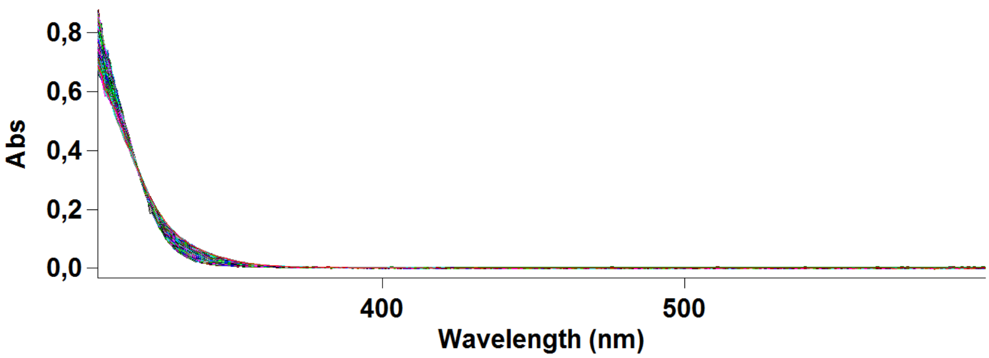

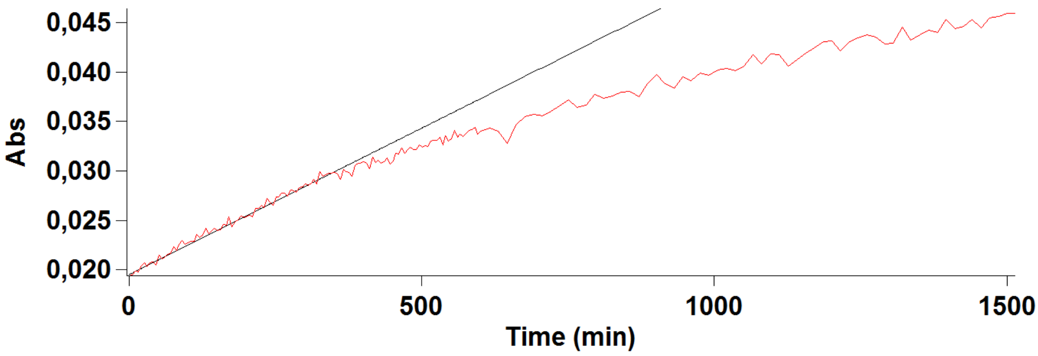

[P5A] = 1.00 x 10^{-4} M

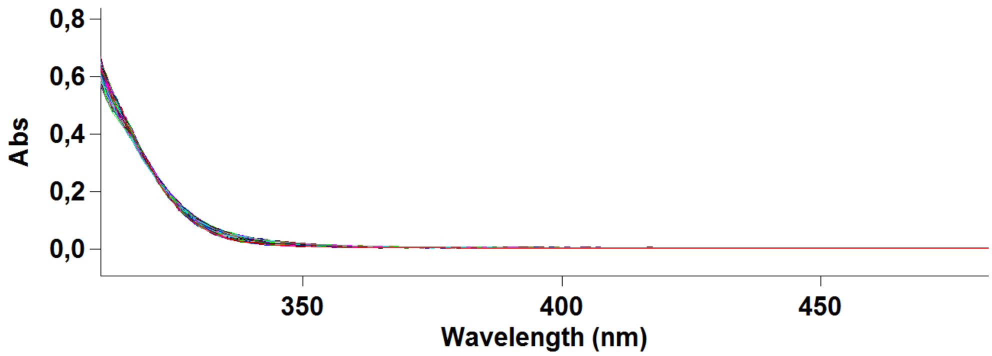

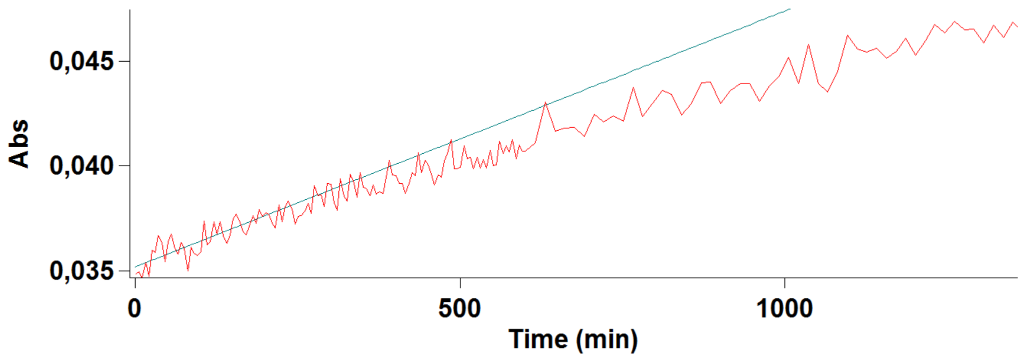

[P5A] = 2.00 x 10^{-4} M

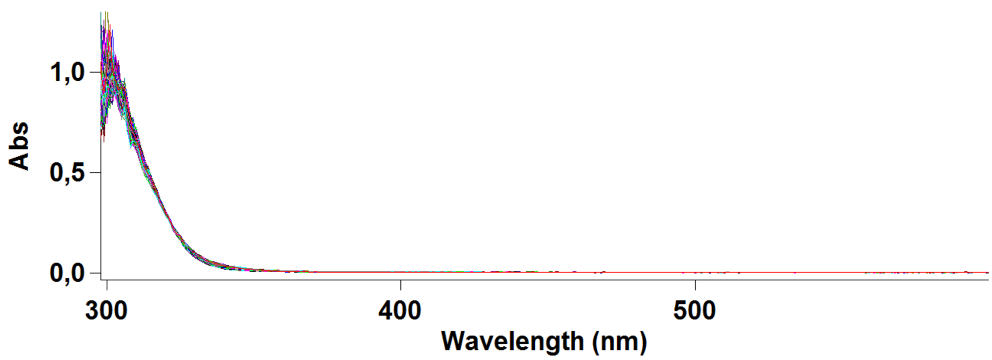

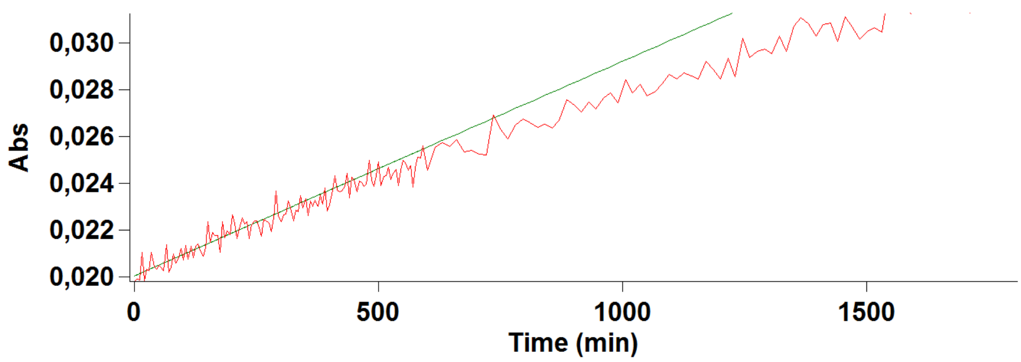

[P5A] = 4.00 x 10^{-4} M

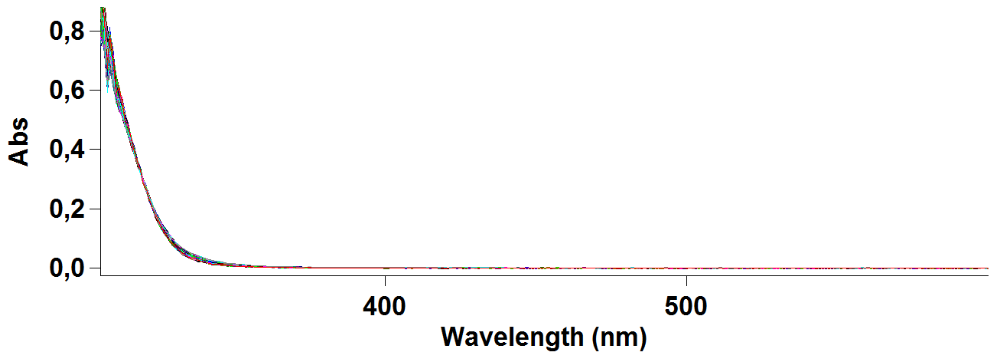

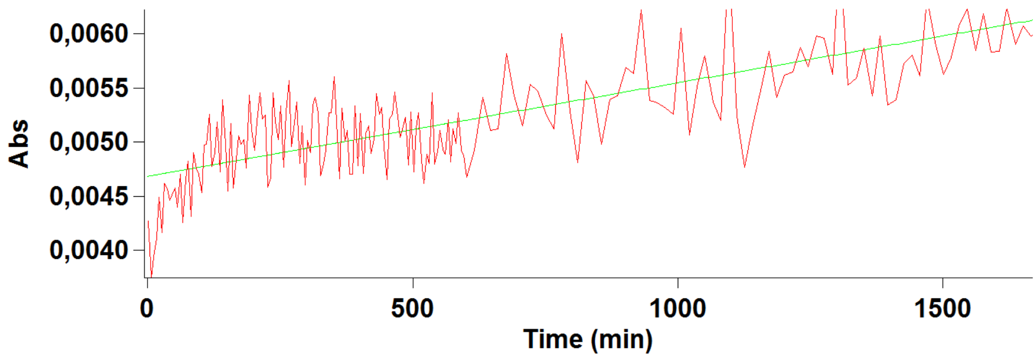

[P5A] = 8.00 x 10^{-4} M

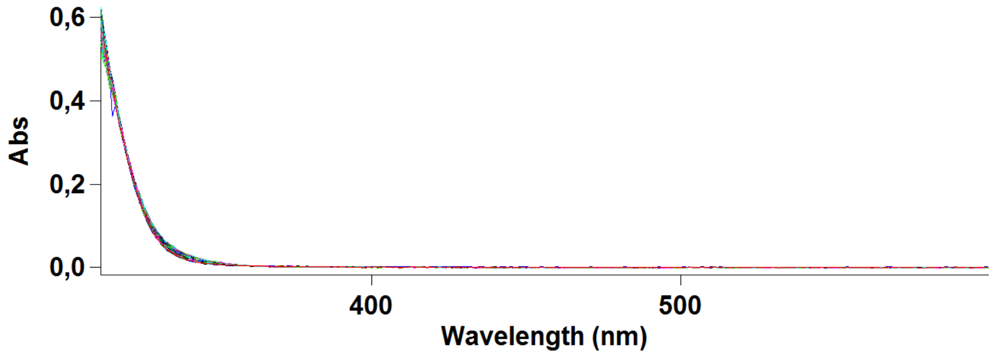

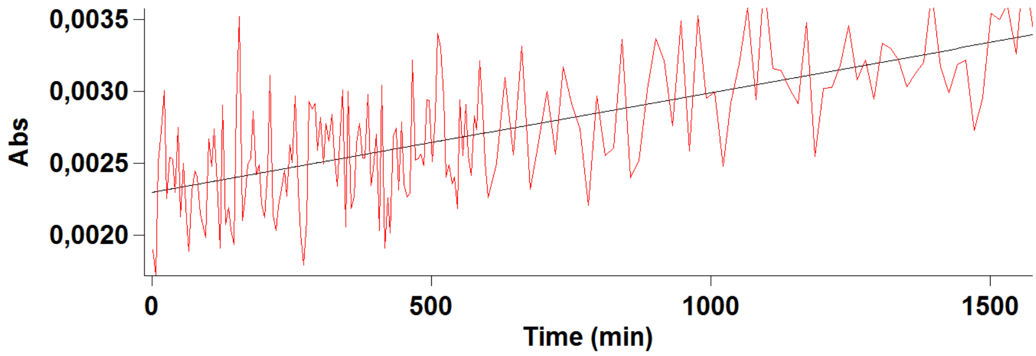

[P5A] = 1.20 X 10^{-3} M

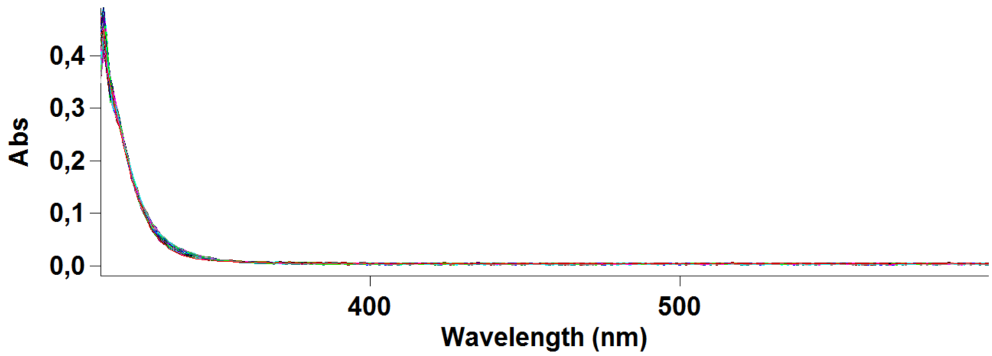

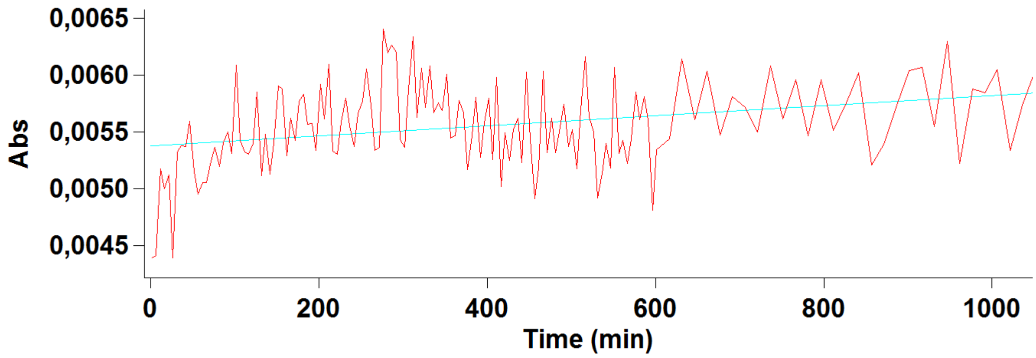

6. Treatment of the kinetic data

6.1 pH-rate profile

The kinetic data of Figure 1A (see manuscript) were fitted using the Equation S1 that describes the observed rate constant (k_{obs}) as a function of the CPA species distribution. We used the same equation to evaluate parameters (rate constants and pK_a) in the P5A cavity. For this, we use excess of P5A to promote total complexation. Scheme 2 (see manuscript) describes all acidity equilibria and rate constants in both environments (H_2O and P5A cavity).

$$k_{obs} = \frac{k_1}{1+\frac{K_{a1}}{[H_3O^+]}+\frac{K_{a1}K_{a2}}{[H_3O^+]^2}} + \frac{k_2}{1+\frac{[H_3O^+]}{K_{a1}}+\frac{K_{a2}}{[H_3O^+]}} + \frac{k_3}{1+\frac{[H_3O^+]}{K_{a2}}+\frac{[H_3O^+]^2}{K_{a1}K_{a2}}} \quad \text{(S1)}$$

k_1, k_2 and k_3 are the rate constants of the neutral ($CPAH_2$), monoanionic ($CPAH^-$) and dianionic (CPA^{2-}) species, respectively; K_{a1} and K_{a2} are the acidity constants.

6.2 Distribution of the CPA species at pHs 2.50, 3.45 and 4.25

Equation S1 determined the values of pK_as in both H_2O and P5A. From this, Table S3 shows the molar fractions of the CPA species as a function of pH, for both environments.

Table S3. Molar fractions of the CPA species at pHs 2.50, 3.45 and 4.25, for both environments.

pH	Environment	$CPAH_2$	$CPAH^-$	CPA^{2-}
2.50	H_2O	85.5 %	13.6 %	0.9 %
	P5A	52.5 %	34.6 %	12.9 %
3.45	H_2O	31.2 %	44.0 %	24.8 %
	P5A	3.8 %	22.3 %	73.9 %
4.25	H_2O	2.4 %	21.5 %	76.1 %
	P5A	0.1 %	4.6 %	95.3 %

6.3 Rate *vs.* P5A concentration

The experiments of k_{obs} *vs.* [P5A] showed inhibitory effects on CPA decomposition, reaching a plateau at approximately 4.0×10^{-4} M (4 equiv). This effect can be explained by the host-guest complexation of CPA in the P5A cavity, with the reaction occurring in both environments (H_2O and P5A). Therefore, the k_{obs} is the sum of the rate constants in both environments weighted by their molar fractions. For this, we consider the possibility of complexation in H:G and H:G_2 stoichiometries for fitting data, as described below:

H:G stoichiometry

$$k_{obs} = k_w X_w + k_{1:1} X_{1:1} \qquad \text{(S2)}$$

$$X_w = \frac{1}{1+K_{1:1}[P5A]} \qquad\qquad X_{1:1} = \frac{K_{1:1}[P5A]}{1+K_{1:1}[P5A]}$$

k_w and $k_{1:1}$ are the rate constants in H_2O and P5A cavity, respectively; X_w and $X_{1:1}$ are the molar fractions of CPA in H_2O and P5A cavity, respectively.

H:G_2 stoichimetry

$$k_{obs} = k_w X_w + k_{1:1} X_{1:1} + k_{1:2} X_{1:2} \qquad \text{(S3)}$$

$$X_w = \frac{1}{1+K_{1:1}[P5A]+K_{1:1}K_{1:2}[P5A]^2}$$

$$X_{1:1} = \frac{K_{1:1}[P5A]}{1+K_{1:1}[P5A]+K_{1:1}K_{1:2}[P5A]^2}$$

$$X_{1:2} = \frac{K_{1:1}K_{1:2}[P5A]^2}{1+K_{1:1}[P5A]+K_{1:1}K_{1:2}[P5A]^2}$$

$k_{1:1}$ and $k_{1:2}$ are the rate constants in the systems H:G and H:G_2, respectively; $X_{1:1}$ and $X_{1:2}$ are the molar fractions of the H:G and H:G_2 complexes, respectively; $K_{1:1}$ and $K_{1:2}$ are the association constants of formation of the H:G and H:G_2 complexes, respectively.

7. NMR experiments

7.1 COSY and HETCOR

The CPA aromatic protons were identify by COSY and HETCOR. Protons derived from anthranilic acid (blue protons) were named H*a*, H*b*, H*c* and H*d*. Protons derived from phthalic anhydride (green protons) were named H*e*, H*f*, H*g* and H*h*.

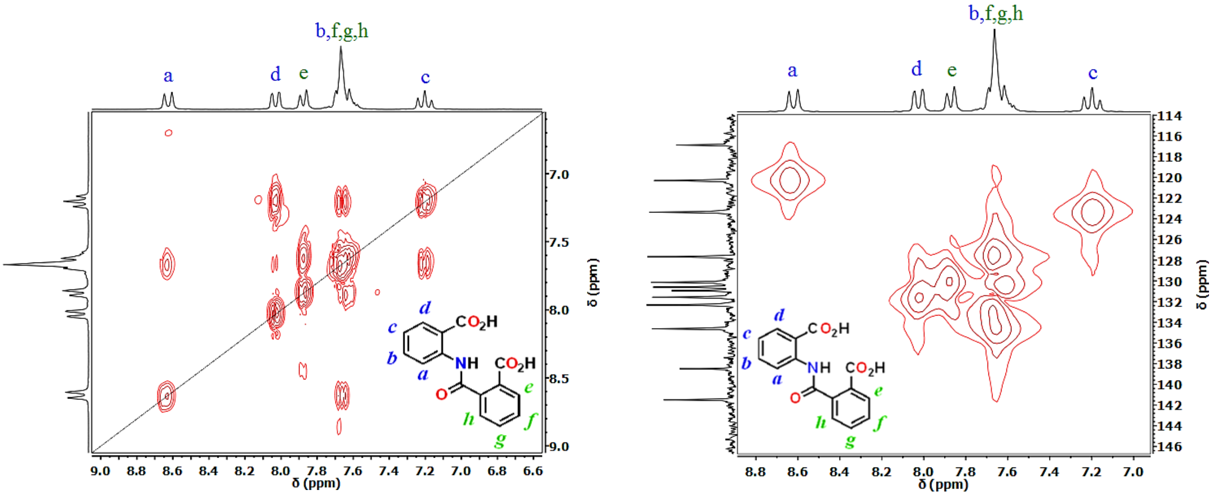

Figure S6 – (**Left**) COSY and (**Right**) HETCOR spectra of CPA (DMSO/TMS, 400 MHz).

7.2 ¹H NMR titration

After identification of all CPA aromatic protons, the ¹H NMR titration were carried out. Figure 4 (see manuscript) shows the chemical shift changes of all CPA aromatic protons in the presence of different P5A equivalents. Figures S7a-b show, in more details, some experimental evidence that complements the discussion in the manuscript. For this, we set the successive spectra in different magnifications for better visualization.

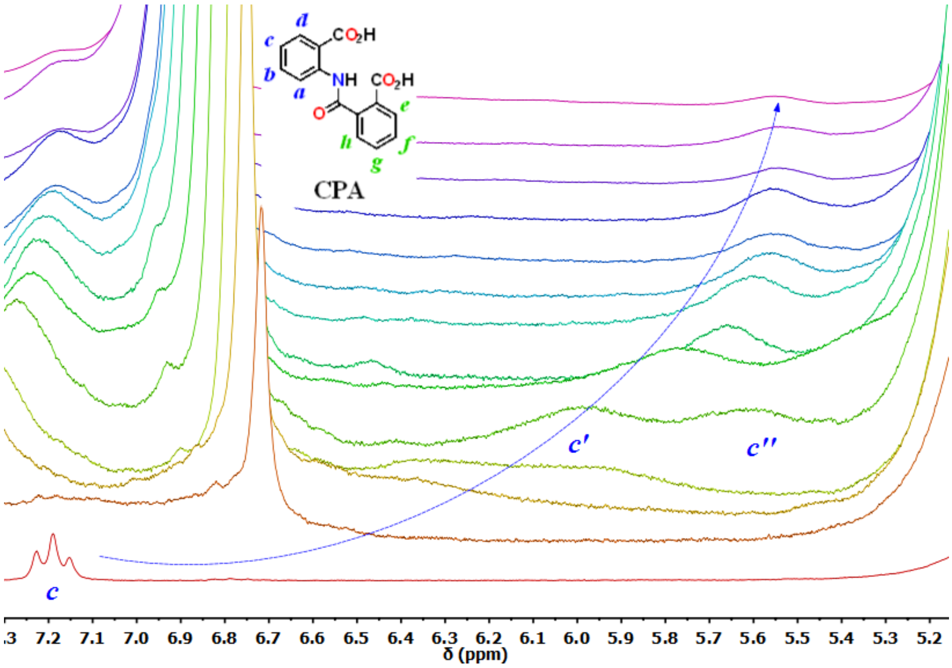

Figure S7a – Splitting of the H*c* proton due to very different environments in asymmetric complexation in $CPA^{2-} \subset P5A \supset CPA^{2-}$ system.

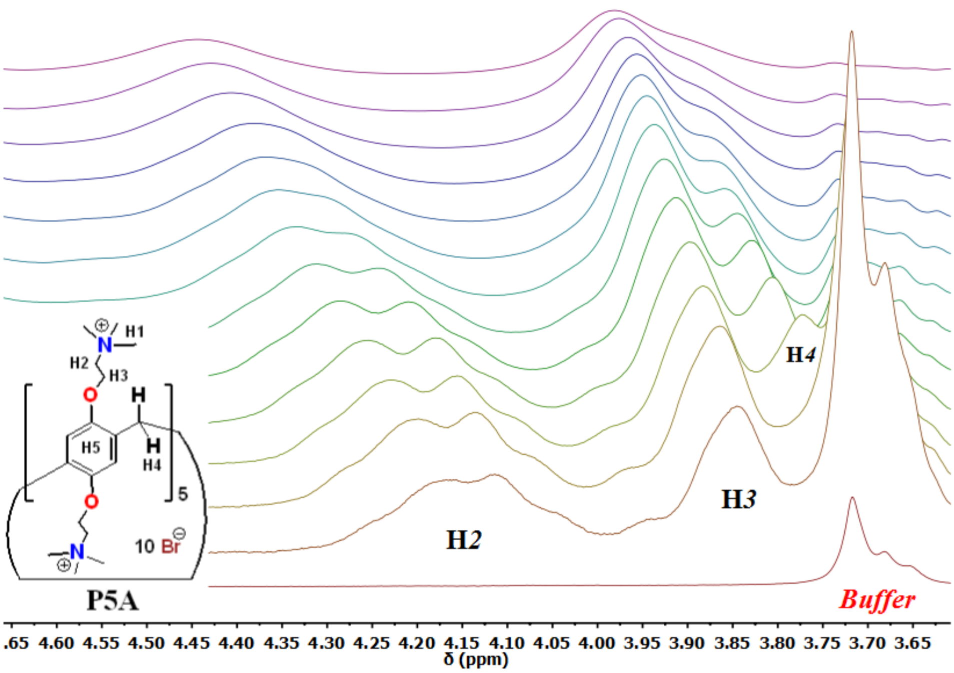

Figure S7b – Splitting of the aliphatic protons of P5A (H*2* >> H*3*) due to very different environments in asymmetric complexation in $CPA^{2-} \subset P5A \supset CPA^{2-}$ system.

Although P6A does not show significant kinetic influence on CPA decomposition, a ^{1}H NMR titration was performed to investigate the formation of host-guest complexes. The data showed very small spectral changes for all CPA protons (Figure S8) as well as large fluctuations in their binding isotherms (Figure S9-Left).

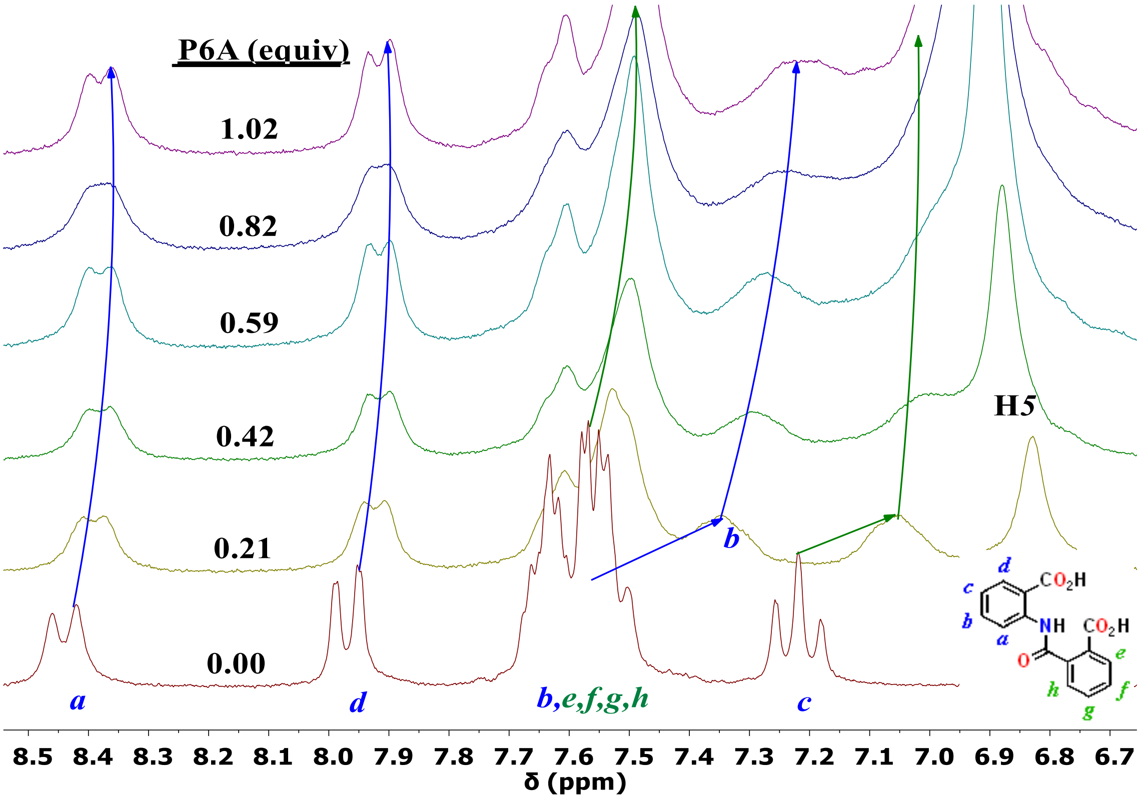

Figure S8 – Chemical shifts of the CPA protons as a function of P6A equivalents (pD 7.0; [Bis-Tris propane] = 0.01 M; 25.0 ºC; 200 MHz).

These data together with the inaccurate saturation of the binding isotherms in $[P6A]_0/[CPA]_0 \cong 0.5$ suggest that two dianionic CPA interact externally with two portals of the P6A. This provides an understanding of the non-formation of host-guest complexes, only interactions external to the P6A cavity with electrostatic interactions acting as the main driving force. This behavior explains the inhibitory effect of only 2.5-fold on the CPA decomposition, where its carboxyl groups remain free to perform intramolecular bifunctional catalysis (Figure S9-Right).

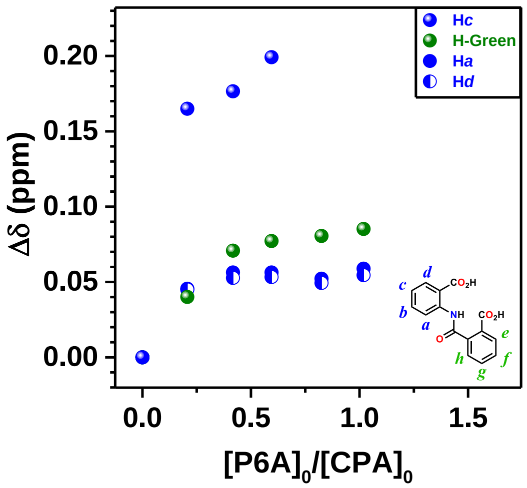

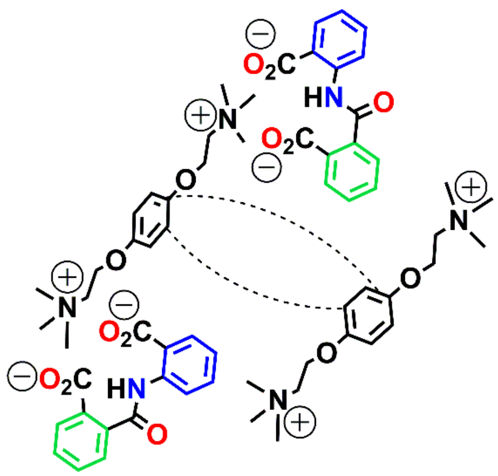

Figure S9 – Δδ *vs*. $[P6A]_0/[CPA]_0$ for CPA protons (**Left**) and one possible structure for external interactions between CPA^{2-} and P6A (**Right**).

7.3 Treatment of the NMR data

The graphics of Δδ *vs*. $[P5A]_0$ were fitted as H:G and $H:G_2$ to investigate the stoichiometry, cooperativity and magnitude of K^G. For this, we use different models,[1] all presented below:

H:G stoichiometry

Assuming only the existence of the H:G complex (H + G $\rightleftharpoons$ H:G), the binding constant is defined by:

$$K_{1:1} = \frac{[\text{H:G}]}{[\text{H}]\cdot[\text{G}]}$$

Due to the free concentrations cannot be measured directly, an alternative approach to use $[P5A]_0$ and $[CPA]_0$ can be solved, reaching:

$$[\text{H:G}] = \frac{1}{2}\left\{[\text{P5A}]_0 + [\text{CPA}]_0 + \frac{1}{K_{1:1}} - \sqrt{\left([\text{P5A}]_0 + [\text{CPA}]_0 + \frac{1}{K_{1:1}}\right)^2 - 4[\text{P5A}]_0[\text{CPA}]_0}\right\}$$

Lastly, the experimental data was fitted with the Equation S4:

$$\Delta\delta = \delta_{1:1}\left(\frac{[\mathrm{H{:}G}]}{[\mathrm{H}]_0}\right) \tag{S4}$$

H:G_2 stoichiometry

Assuming the existence of high order complexes (H + G $\rightleftharpoons$ H:G + G $\rightleftharpoons$ H:G_2), the macroscopic binding constants are defined by:

$$K_{1:1} = \frac{[\mathrm{H{:}G}]}{[\mathrm{H}]\cdot[\mathrm{G}]} \qquad K_{1:2} = \frac{[\mathrm{H{:}G_2}]}{[\mathrm{H{:}G}]\cdot[\mathrm{G}]}$$

Thus, the free CPA concentration can be determined by the cubic equation below:

$$a[\mathrm{CPA}]^3 + b[\mathrm{CPA}]^2 + c[\mathrm{CPA}] - [\mathrm{CPA}]_0 = 0$$

Where:

$$a = K_{1:1}K_{1:2}$$

$$b = K_{1:1}(2K_{1:2}[\mathrm{P5A}]_0 - K_{1:2}[\mathrm{CPA}]_0 + 1)$$

$$c = K_{1:1}([\mathrm{P5A}]_0 - [\mathrm{CPA}]_0) + 1$$

Lastly, the experimental data was fitted with the Equation S5:

$$\Delta\delta = \frac{\delta_{1:1}K_{1:1}[\mathrm{CPA}] + \delta_{1:2}K_{1:1}K_{1:2}[\mathrm{CPA}]^2}{1 + K_{1:1}[\mathrm{CPA}] + K_{1:1}K_{1:2}[\mathrm{CPA}]^2} \tag{S5}$$

For fitting data in H:G_2 stoichiometry we used the BindFit online tool. Table S4 shows the values of $K_{1:1}$ and $K_{1:2}$ for all CPA protons. As mentioned in the manuscript, these data were treated qualitatively due to the relationship $K_{1:1} << K_{1:2}$ being able to generate errors and negative coefficient to H:G stoichiometry ($-\delta_{1:1}$).[2] To access each data file click in BindFit (blue link).

Table S4. Equilibrium constants for all CPA^{2-} protons obtained from fitting experimental data to Equation S5 (using BindFit online tool, supramolecular.org).

Proton	**Link**	**$K_{1:1}$ (M^{-1})**	**$K_{1:2}$ (M^{-1})**
a	BindFit	$1.21 \times 10^{-2} \pm 2.9\%$	$8.45 \times 10^{4} \pm 1.7\%$
b	BindFit	$4.21 \times 10^{-2} \pm 3.3\%$	$1.41 \times 10^{5} \pm 2.3\%$
c	BindFit	$6.00 \times 10^{-2} \pm 15.7\%$	$3.11 \times 10^{5} \pm 11.8\%$
d	BindFit	$7.17 \times 10^{-3} \pm 1.4\%$	$1.72 \times 10^{5} \pm 0.8\%$
e-h	BindFit	$2.03 \times 10^{-2} \pm 9.1\%$	$4.22 \times 10^{5} \pm 6.8\%$
N-H	BindFit	$1.32 \times 10^{-2} \pm 5.7\%$	$3.42 \times 10^{5} \pm 4.1\%$

8. References

(1) Thordarson, P. Determining Association Constants from Titration Experiments in Supramolecular Chemistry. *Chem. Soc. Rev.* **2011**, *40* (3), 1305–1323.

(2) Dodziuk, H.; Nowinski, K. S.; Kozminski, W.; Dolgonos, G. On the Impossibility of Determination of Stepwise Binding Constants for the 1 : 2 Complex of (+)-Camphor with α-Cyclodextrin. *Org. Biomol. Chem.* **2003**, *1* (3), 581–584.